Dynamics of Atmospheres and Oceans, 10 (1986) 185–219
Elsevier Science Publishers B.V., Amsterdam – Printed in The Netherlands

QUASIGEOSTROPHIC ENERGETICS OF OPEN OCEAN REGIONS

NADIA PINARDI and ALLAN R. ROBINSON

Center for Earth and Planetary Physics, Harvard University, Cambridge, MA 02128 (U.S.A.)

(Received October 7, 1985; accepted March 21, 1986)

ABSTRACT

Pinardi, N. and Robinson, A.R., 1986. Quasigeostrophic energetics of open ocean regions. Dyn. Atmos. Oceans, 10: 185–219.

We present a method for local energy and vorticity analysis (EVA) of open regions of oceanic flow governed by quasigeostrophic dynamics. The purpose is to infer from real and simulated data sets the physics of synoptic/mesoscale processes, and to identify general signatures of such processes. We first derive, via a Rossby number expansion, the form of the local conservation law for quasigeostrophic energy density in terms of the geostrophic pressure field. We relate the quasigeostrophic terms to their more general form and also identify the different local ageostrophic contributions to the pressure work flux divergences. Analysis methods include time series of maps of terms, space-time integral time series, and schematic open region diagrams. Rossby wave and normal mode barotropic and baroclinic instability processes are studied in open regions, and local conversion/transport properties are defined. It is found that the instability process is indicated by both Reynolds-stress-like terms (ΔF_κ, ΔF_A) and ageostrophic pressure work divergence (ΔF_π^a, δf_π^a). The process of local growth of energy is indicated by the local growth of asymmetries in the divergence terms. The application of EVA to real data situations which are made self-consistent by quasigeostrophic filtering is introduced. Real data initialization of a quasigeostrophic dynamical model provides the required dynamical interpolation procedure. Finally an eddy merger event captured during a successful dynamical forecast in the California Current region (Robinson et al.) is described and interpreted via EVA.

1. INTRODUCTION

The energetic balances of the oceans have been studied extensively in recent years. The studies have been predominantly with primitive equation dynamics and in closed basins. Some research has been initiated for open subregions and also for quasigeostrophic dynamics but with basin integrated energetics (e.g., Haidvogel and Holland, 1978; Harrison and Robinson, 1978; Harrison, 1979). Oceanographers are of course building on the experience of fundamental atmospheric concepts and studies (Lorenz, 1967; Van

0377-0265/86/$03.50

Mieghem, 1973) and recent studies share some common concerns (Plumb, 1983). Here we treat formally the local, nonintegrated energetics of arbitrary open regional quasigeostrophic systems. The ocean is of course spatially inhomogeneous in its dynamics. Also, interesting intensive data sets exist only for limited areas. Our motivation is to be able to deduce local dynamical processes from regional data sets, both real oceanic and numerically simulated. Many processes are now known to be quasigeostrophic, and quasigeostrophic modeling is prevalent. As developed below, we will subject real data sets to a quasigeostrophic dynamical filter, before taking the higher derivatives required for energy balance estimates.

We first derive quasigeostrophic local energy equations for open boundary systems in a self-consistent way, i.e., expressing all the energy fluxes and their divergences in terms of the quasigeostrophic streamfunction field. The approach simply parallels the familiar vorticity equation derivation; we work through first order equations but eliminate first order fields.

An important aim is to interpret the energy dynamics of quasigeostrophic open ocean systems and to relate the somewhat unfamiliar expressions which arise to more familiar forms, e.g., those of the primitive equations. Furthermore, since geostrophic flows have a divergenceless energy flux, it is of interest to identify the ageostrophic effect which gives rise to a local energy source.

We next study the signatures of basic baroclinic and barotropic instabilities, processes that occur in quasigeostrophic systems as an aid to the understanding of the finite amplitude processes using the local energy equations. Finally we illustrate the application of this approach to a real ocean data study. The horizontal and vertical resolution of measurements is usually poor even in regions with relatively more accurate and intensive data sets (MODE, POLYMODE); direct evaluation of high order derivatives as they appear in the energy equations is usually precluded except for a very few 'point' experiments (Bryden, 1982; McWilliams et al., 1983). We show that the use of a dynamical interpolation scheme as provided by a numerical model which assimilates the data, adjusts the fields in such a way that a consistent diagnostic study of the energy and vorticity dynamics can be achieved. Thus definite and unambiguous dynamical processes can be elucidated for fields with the general features of the observed fields. To the extent that quasigeostrophic dynamics is an accurate physical model, these processes will be relevant to real ocean dynamics.

In section 2 we introduce the energy equations for a Boussinesq incompressible flow, and in section 3 we derive the self-consistent energy equations in the quasigeostrophic approximation which are summarized in section 4. Section 5 analyzes Rossby-wave propagation, section 6 the local energetics of baroclinically unstable Eady waves, and section 7 the barotropic instability of a linear zonal shear flow between two regions of uniform flow. In section 8 an example of dynamically interpolated field of eddies and jets in the California Current system (Robinson et al., 1985a, b) is analyzed and local conversions of energy are interpreted during a process of barotropic finite amplitude instability.

2. THE ENERGY EQUATIONS

Consider the three-dimensional momentum and thermodynamical equations for an ideal hydrostatic, Boussinesq incompressible fluid in a rectangular β-plane system of coordinates (x, y, z) with u, v, w the eastward, northward and vertical velocity components, $f = f_0 + \beta_0(y - y_0)$, and y_0 the central latitude. Let ρ be the total density, ρ_0 its volume and time average, g the gravitational acceleration, and P the pressure.

Let the density and pressure fields be divided into a basic motionless state $\tilde{\rho}(z)$ and $\tilde{p}(z)$ independent of x, y, t, and dynamical perturbation fields $\Delta(x, y, z, t)$ and $p(x, y, z, t)$, i.e.

$$P(x, y, z, t) = \tilde{p}(z) + p(x, y, z, t) = -\rho_0 \int^z g\tilde{\rho}(z')\,\mathrm{d}z' + p(x, y, z, t) \tag{1a}$$

$$\rho(x, y, z, t) = \tilde{\rho}(z)\rho_0 - \rho_0\,\Delta(x, y, z, t) \tag{1b}$$

This basic state is defined to be the long time horizontal space average for the open domain subregion of the ocean which we are interested in studying. In many open ocean regions of interest, the decomposition of the field variables in (1) is consistent with data over $O(10^2 - 10^3$ km). By our convention, any steady regional flow will contribute to the perturbation dynamical variables, p and Δ. The equations for momentum, mass and density anomaly are

$$\frac{\partial u}{\partial t} + u\frac{\partial u}{\partial x} + v\frac{\partial u}{\partial y} + w\frac{\partial u}{\partial z} - fv = -\frac{p_x}{\rho_0} \tag{2a}$$

$$\frac{\partial v}{\partial t} + u\frac{\partial v}{\partial x} + v\frac{\partial v}{\partial y} + w\frac{\partial v}{\partial z} + fu = -\frac{p_y}{\rho_0} \tag{2b}$$

$$0 = -\frac{p_z}{\rho_0} + \Delta g \tag{2c}$$

$$u_x + v_y + w_z = 0 \tag{2d}$$

$$\frac{\partial \Delta}{\partial t} + u\frac{\partial \Delta}{\partial x} + v\frac{\partial \Delta}{\partial y} + w\frac{\partial \Delta}{\partial z} - w\frac{\partial \tilde{\rho}}{\partial z} = 0 \tag{2e}$$

Equations 2 regarded as a general dynamical system have associated first integrals of motion which are the quadratic invariants called kinetic energy and available potential energy. The total kinetic energy equation is obtained by multiplying eqs. 2a–c by u, v, w, respectively, and summing them; the multiplication of (2c) by w produces the total pressure work flux, but the approximate hydrostatic balance eliminates the $w^2/2$ contribution to the kinetic energy. From a physical energy viewpoint, since the motion is divergenceless, the internal energy does not change by mechanical work and the potential energy is only gravitational energy. The available gravitational energy equation is obtained multiplying (2e) by $-(\rho_0 g\,\Delta)/[(\partial\tilde{\rho}/\partial z)]$. The weighting factor for the Δ^2 energy is chosen to allow buoyancy work conversion between the two energies. We obtain

$$\rho_0 \frac{\partial}{\partial t}\left(\frac{u^2+v^2}{2}\right) = -\rho_0 \nabla \cdot \left[\vec{\mathbf{u}}\left(\frac{u^2+v^2}{2}\right)\right] - \nabla \cdot (p\vec{\mathbf{u}}) + \rho_0 g\,\Delta w \tag{3a}$$

$$\rho_0 \frac{\partial}{\partial t}\left(\frac{g\,\Delta^2}{2s}\right) = -\rho_0 \nabla \cdot \left[\vec{\mathbf{u}}\left(\frac{g\,\Delta^2}{2s}\right)\right] - \frac{\rho_0 g\,\Delta^2}{2s^2} w \frac{\partial s}{\partial z} - \rho_0 g\,\Delta w \tag{3b}$$

where $s = -(\partial\tilde{\rho})/(\partial z)$.

Lorenz (1955) first derived a version of (3b), Bray and Fofonoff (1981) discussed the consistency of the definition of $\tilde{\rho}$ and the evaluation of Δ^2/s from real ocean data, and Holliday and McIntyre (1981) also took the quadratic invariant viewpoint.

The time rate of change of the kinetic energy density $K \equiv (u^2+v^2)/2$ is due to advection of K in and out of the region (advective working rate), to the rate of doing work by the fluid against the pressure force (pressure working rate) and to the negative of the buoyancy working rate. The time rate of change of the available gravitational energy $A \equiv g\,\Delta^2/2s$ is due to advection of gravitational energy in and out of the region (advective working rate), to the buoyancy working rate and to an apparent source or sink due to the shear in the basic stability profile. The buoyancy working rate is now seen to be a conversion term between K and A since it appears in eqs. 3a and 3b with opposite signs. The term $-\vec{\mathbf{u}}\cdot\nabla p$ has been equivalently written as $-\nabla\cdot(p\vec{\mathbf{u}})$ since the motion is divergenceless.

Finally, we nondimensionalize the variables and equations using the following time, velocity and length scales

$$\begin{aligned}
&(x, y) = D(x', y') \quad z = Hz' \quad t = t_0 t' \\
&(u, v) = V_0(u', v') \quad w = \frac{H}{D} V_0 w' \\
&p = V_0 f_0 \rho_0 D p' \quad \Delta = \frac{f_0 V_0 D}{gH}\delta
\end{aligned} \tag{4}$$

TABLE I

Nondimensional parameter	Expression	Comment
ϵ	$\epsilon = \frac{1}{f_0 t_0}$	Ratio of local rotation period $T = 1/f_0$ to time scale t_0
α	$\alpha = t_0 \frac{V_0}{D}$	Ratio of time scale t_0 to advective time scale $t_A = D/V_0$
Γ^2	$\frac{f_0^2 D^2}{N_0^2 H^2}$	Rotational internal Froude number
σ	$\sigma = \frac{N_0^2}{N^2(z)}$	Stability parameter; $N^2(z) = -g\,\partial\tilde{\rho}/\partial z$; N_0^2 characteristic buoyancy frequency
β	$\beta = \beta_0 t_0 D$	Ratio of planetary Rossby wave time scale, $t_\beta = (\beta_0 D)^{-1}$ to time scale t_0; $\beta_0 = \frac{2\Omega \cos\theta_0}{r}$ r = radius of the Earth

Upon dropping the primes, eqs. 3a and 3b become in nondimensional form

$$\epsilon \frac{\partial}{\partial t} \frac{(u^2 + v^2)}{2} = -\epsilon\alpha \nabla \cdot \left(\vec{\mathbf{u}} \frac{(u^2 + v^2)}{2} \right) - \nabla \cdot (p\vec{\mathbf{u}}) + \delta w \tag{5}$$

$$\epsilon\Gamma^2 \frac{\partial}{\partial t} \left(\sigma \frac{\delta^2}{2} \right) = -\epsilon\alpha\Gamma^2 \nabla \cdot \left(\vec{\mathbf{u}}\sigma \frac{\delta^2}{2} \right) - \epsilon\alpha\Gamma^2 \sigma \frac{\delta^2}{2s} w \frac{\partial s}{\partial z} - \delta w \tag{6}$$

The parameters in eqs. 5 and 6 are

$$\epsilon = \frac{1}{f_0 t_0} \quad \alpha = \frac{V_0}{D} t_0 \quad \sigma = \frac{N_0^2}{N^2(z)} \quad \Gamma^2 = \frac{f_0^2 D^2}{N_0^2 H^2}$$

which are also listed in Table I. The Rossby number of our system is chosen to be ϵ which is assumed to be much less than one; α, the ratio of imposed and advective time scales, and Γ^2, the squared ratio of the horizontal length scale to the characteristic internal deformation radius, are taken to be 0(1).

We now write eqs. 5 and 6 symbolically and identify the physical terms and symbols in Table II. These equations result

$$\dot{K} = \Delta F_\kappa + \delta f_\kappa + \Delta F_\pi + \delta f_\pi - b \tag{7a}$$

$$\dot{A} = \Delta F_A + \delta f_A + \delta s + b \tag{7b}$$

TABLE II

Energy equations symbols

Symbol	Physical process	Dimensional form	Nondimensional form
K	Kinetic energy density	$\frac{u^2+v^2}{2}$	$\frac{u^2+v^2}{2}$
A	Available gravitational energy density (A.G.E.)	$\frac{g}{\hat{s}}\frac{\Delta^2}{2}$	$\sigma\Gamma^2\frac{\delta^2}{2}$
$\vec{\pi}$	Pressure energy fluxes	$p\vec{\mathbf{u}}$	$p\vec{\mathbf{u}}$
$\dot{K}$	Time rate of change of K	$\frac{\partial}{\partial t}K$	$\epsilon\frac{\partial}{\partial t}K$
ΔF_k	Horizontal kinetic energy *advective* working rate	$-\frac{\partial}{\partial x}(uK)-\frac{\partial}{\partial y}(vK)$	$-\epsilon\alpha\frac{\partial}{\partial x}(uK)-\epsilon\alpha\frac{\partial}{\partial y}(vK)$
δf_k	Vertical kinetic energy *advective* working rate	$-\frac{\partial}{\partial z}(wK)$	$-\epsilon\alpha\frac{\partial}{\partial z}(wK)$
ΔF_π	Horizontal *pressure* working rate	$-\frac{\partial}{\partial x}(pu)-\frac{\partial}{\partial y}(pv)$	$-\frac{\partial}{\partial x}(pu)-\frac{\partial}{\partial y}(pv)$

δf_π	Vertical *pressure* working rate	$-\frac{\partial}{\partial z}(pw)$	$-\frac{\partial}{\partial z}(pw)$
b	Buoyancy work or interaction working rate	$-\rho_0 \Delta g w$	$-\delta w$
$\dot{A}$	Time rate of change of A	$\frac{\partial}{\partial t}A$	$\epsilon\frac{\partial}{\partial t}A$
ΔF_A	Horizontal A.G.E. *advective* working rate	$-\frac{\partial}{\partial x}(uA)-\frac{\partial}{\partial y}(vA)$	$-\epsilon\alpha\frac{\partial}{\partial x}(uA)-\epsilon\alpha\frac{\partial}{\partial y}(vA)$
δf_A	Vertical A.G.E. *advective* working rate	$-\frac{\partial}{\partial z}(wA)$	$-\epsilon\alpha\frac{\partial}{\partial z}(wA)$
δs	Apparent source or sink of A.G.E. due to stationary shear	$-\frac{w\rho_0 g\Delta^2}{2s^2}\frac{\partial s}{\partial z}$	$-\epsilon\alpha\Gamma^2\sigma\frac{\delta^2}{2s}w\frac{\partial s}{\partial z}$

3. QUASIGEOSTROPHIC ENERGETICS

3.1. The Rossby number expansion of the energy equations

We now expand δ, p, u, v, w in the Rossby number ϵ. The subscripts indicate the order in the expansion and w_0 is taken to be zero. Henceforth, the vector arrows and the gradient operator, ∇, will denote two-dimensional quantities.

The zeroth order Rossby number expansion of the kinetic energy equation (5) is the diagnostic relationship $\nabla \cdot (p_0\vec{\mathbf{u}}_0) = 0$ which is the well-known statement that the pressure energy flux by completely geostrophic motions does not diverge or change the kinetic energy density. Generally of course the kinetic energy equation is always determined by less than a divergenceless vector, and the zeroth order kinetic energy equation is degenerate in that it contains no useful information beyond the constraint of geostrophy. As in the case of vorticity dynamics we have to go to the first order expansion in order to find a prognostic equation for the kinetic energy density of the geostrophic field $K_0 = 1/2(u_0^2 + v_0^2$ and the available gravitational energy density of the geostrophic field $A_0 = \sigma\Gamma^2(\delta_0^2/2)$.

The first order contributions to (5) and (6) are

$$\frac{\partial}{\partial t}K_0 = -\alpha\nabla\cdot(\vec{\mathbf{u}}_0K_0) - \nabla\cdot(p_1\vec{\mathbf{u}}_0 + p_0\vec{\mathbf{u}}_1) - (p_0w_1)_z + \delta_0w_1 \tag{8a}$$

$$[\dot{K}]_0 = \Delta[F_\kappa]_0 + 0 + \Delta[F_\pi]_1 + \delta[f_\pi]_1 - [b]_1 \tag{8b}$$

$$\dot{K} = \Delta F_\kappa + \delta f_\kappa + \Delta F_\pi + \delta f_\pi - b \tag{7a}$$

$$\frac{\partial}{\partial t}A_0 = -\alpha\nabla\cdot(\vec{\mathbf{u}}_0A_0) - \delta_0w_1 \tag{9a}$$

$$[\dot{A}]_0 = \Delta[F_A]_0 + 0 + 0 + [b]_1 \tag{9b}$$

$$\dot{A} = \Delta F_A + \delta f_A + \delta s + b \tag{7b}$$

Equations 8 and 9 are our fundamental kinetic and available gravitational energy density equations. The (a) versions show the detailed expansion structure of the contributing terms, and the (b) versions represent these schematically to facilitate comparison to the full eqs. 7a and 7b. Henceforth for convenience we drop the subscripts from eqs. 8b and 9b.

Each term in eqs. 8 and 9 is of course an 0(1) quantity. Thus the physically small ageostrophic vertical velocity can do important work against the vertical pressure gradients to this order although it cannot advect the geostrophic kinetic energy.

3.2. Elimination of fields not derivable from p_0

Equation 8 contains the ageostrophic pressure work flux which we indicate by

$$\vec{\pi}_1 = p_0\vec{\mathbf{u}}_1 + \vec{\mathbf{u}}_0 p_1 + \hat{k} p_0 w_1 \tag{10}$$

where $\hat{k}$ is the unit vector in the z direction.

To further decompose $\vec{\pi}_1$ and to express it in terms of p_0, we use the familiar first order Rossby number expansions of the momentum and thermodynamical equations, viz.

$$v_1 = u_{0t} + \alpha\vec{\mathbf{u}}_0 \cdot \nabla u_0 - \beta y v_0 + p_{1x} \tag{11a}$$

$$u_1 = -v_{0t} - \alpha\vec{\mathbf{u}}_0 \cdot \nabla v_0 - \beta y u_0 - p_{1y} \tag{11b}$$

$$w_1 = -\sigma\Gamma^2 p_{0zt} - \alpha\Gamma^2\vec{\mathbf{u}}_0 \cdot \nabla(\sigma p_{0z}) \tag{12}$$

where β is listed in Table I and is 0(1). In eq. 12 the hydrostatic relationship $\delta_0 = p_{0z}$ has been used. Cross-differentiating (11a, b) and using (12), yields the well known prognostic equation for the dynamical vorticity, q

$$\begin{aligned}\partial_t q &= \partial_t \nabla^2 p_0 + \Gamma^2\, \partial_t(\sigma p_{0z})_z \\ &= -\alpha\nabla \cdot \left(\vec{\mathbf{u}}_0 \nabla^2 p_0\right) - \alpha\Gamma^2\, \nabla \cdot \left(\vec{\mathbf{u}}_0(\sigma p_{0z})_z\right) - \beta p_{0x}\end{aligned} \tag{13a}$$

$$\dot{Q} = \dot{R} + \dot{T} = \Delta F_R + \Delta F_T + \Delta F_P \tag{13b}$$

$$Q = \nabla^2 p_0 + \Gamma^2(\sigma p_{0z})_z = R + T \tag{13c}$$

In Table III the symbols denoting the terms in eq. 13 are elucidated.

We insert (11a, b) and (12) in the definition of $\vec{\pi}_1$ and obtain

$$\begin{aligned}\vec{\pi}_1 = {} & \hat{i}\left[-p_0 v_{0t} - \alpha p_0\vec{\mathbf{u}}_0 \cdot \nabla v_0 - \beta y u_0 p_0 - p_{1y} p_0 + p_1 u_0\right] \\ & + \hat{j}\left[p_0 u_{0t} + \alpha p_0 \vec{\mathbf{u}}_0 \cdot \nabla u_0 - \beta y v_0 p_0 + p_{1x} p_0 + p_1 v_0\right] \\ & - \hat{k}\left[p_0 \Gamma^2 \sigma p_{0zt} + p_0 \alpha \Gamma^2 \vec{\mathbf{u}}_0 \cdot \nabla(\sigma p_{0z})\right]\end{aligned}$$

$$\vec{\pi}_1 = \hat{i}\left[p_0 u_1 + p_1 u_0\right] + \hat{j}\left[p_0 v_1 + p_1 v_0\right] + \hat{k} p_0 w_1 \tag{15}$$

where $\hat{\mathrm{i}}$, $\hat{\mathrm{j}}$ are the unit vectors in the x, y directions, respectively.

The pressure work flux $\vec{\pi}_1$ still contains p_1 but since these terms are divergenceless, i.e., $\partial_x(p_{1y} p_0 + p_1 p_{0y}) = \partial_y(p_{1x} p_0 + p_1 p_{0x})$ they do not contribute to the energy working rate.

It is possible now to rewrite (8a) as

$$\begin{aligned}\frac{\partial}{\partial t} K_0 = {} & -\alpha \nabla \cdot (\vec{\mathbf{u}}_0 K_0) - \nabla \cdot \left(p_0 \hat{\mathrm{K}} \times \vec{\mathbf{u}}_{0t} + \alpha p_0 \vec{\mathbf{u}}_0 \cdot \nabla(\hat{\mathrm{K}} \times \vec{\mathbf{u}}_0) - \beta y p_0 \vec{\mathbf{u}}_0\right) \\ & + \left(p_0 \sigma \Gamma^2 p_{0zt} + p_0 \alpha \Gamma^2 \sigma \vec{\mathbf{u}}_0 \cdot \nabla p_{0z}\right)_z + \delta_0 w_1\end{aligned} \tag{16a}$$

TABLE III

Pseudopotential vorticity terms

Symbol	Physical process	Term
Q	Dynamical vorticity	$\Gamma^2(\sigma p_z)_z + \nabla^2 p$
T	Thermal vorticity	$\Gamma^2(\sigma p_z)_z$
R	Relative vorticity	$\nabla^2 p$
$\dot{R}$	Time rate of change of relative vorticity	$\frac{\partial}{\partial t}\nabla^2 p$
$\dot{T}$	Time rate of change of thermal vorticity	$\Gamma^2 \frac{\partial}{\partial t}(\sigma p_z)_z$
ΔF_R	Divergence of relative vorticity advective flux	$-\alpha\vec{v}\cdot\nabla(\nabla^2 p)$
ΔF_T	Divergence of thermal vorticity advective flux	$-\alpha\Gamma^2\vec{v}\cdot\nabla(\sigma p_z)_z$
ΔF_P	Divergence of planetary vorticity	$-\beta p_x$

$$\dot{K} = \Delta F_\kappa + \Delta F_\pi + \delta f_\pi - b \tag{8b}$$

$$\dot{K} = \Delta F_\kappa + \Delta F_\pi^t + \Delta F_\pi^a + \Delta F_\pi^\beta + \delta f_\pi^t + \delta f_\pi^a - b \tag{16b}$$

In eq. 16b we have indicated the several components of ΔF_π and δf_π: they are also listed in Table IV together with their physical meaning and are further decomposed into terms associated with meridional and zonal components.

We now elucidate the relationship between vorticity dynamics and transport terms in the energy equations. The total energy density equation can be expressed as the sum of 9 and 16 with $\hat{k} \times \vec{\mathbf{u}}_0 = -\nabla p_0$ substituted, viz.

$$\begin{aligned}\frac{\partial}{\partial t}(K_0 + A_0) = {} & -\alpha\nabla\cdot(\vec{\mathbf{u}}_0(K_0 + A_0)) + \nabla\cdot(p_0\alpha\vec{\mathbf{u}}_0\cdot\nabla(\nabla p_0)) \\ & + \nabla\cdot(\beta y p_0\vec{\mathbf{u}}_0) + \partial_z(p_0\alpha\sigma\Gamma^2\vec{\mathbf{u}}_0\cdot\nabla p_{0z}) + \nabla\cdot(p_0\nabla p_{0t}) \\ & + \partial_z(p_0\Gamma^2\sigma p_{0zt})\end{aligned} \tag{17a}$$

$$\dot{K} + \dot{A} = \Delta F_\kappa + \Delta F_A + \Delta F_\pi^a + \Delta F_\pi^\beta + \delta f_\pi^a + \Delta F_\pi^t + \delta f_\pi^t \tag{17b}$$

The right hand side of eq. 17 can be expressed as $-\nabla_3\cdot\vec{\mathbf{F}}$ where $(\nabla_3\cdot)$ is the three-dimensional divergence operator and $\vec{\mathbf{F}}$ the 3-dimensional total energy flux vector

$$\vec{\mathbf{F}} = \alpha(\vec{\mathbf{u}}_0 A_0 + \vec{\mathbf{u}}_0 K_0) - p_0\nabla p_{0t} - \alpha p_0\vec{\mathbf{u}}_0\cdot\nabla\nabla p_0 - \frac{\beta p_0^2}{2}\hat{i} + \hat{k}p_0 w_1 \tag{18a}$$

$$\vec{\mathbf{F}} = \vec{\mathbf{F}}_A + \vec{\mathbf{F}}_\kappa + \vec{\mathbf{F}}_\pi^t + \vec{\mathbf{F}}_\pi^a + \vec{\mathbf{F}}_\pi^\beta + \vec{\mathbf{f}}_\pi \tag{18b}$$

TABLE IV
Quasigeostrophic energy equations symbols

Symbol	Physical process	Term
$\Delta_x F_\pi^t$	Zonal pressure working rate due to acceleration of the meridional geostrophic velocity	$\partial_x(pp_{xt}) = \partial_x(pv_t)$
$\Delta_y F_\pi^t$	Meridional pressure working rate due to acceleration of the zonal geostrophic velocity	$\partial_y(pp_{yt}) = -\partial_y(pu_t)$
$\Delta_y F_\pi^a$	Meridional pressure working rate due to advection of the zonal geostrophic velocity	$-\partial_y(p\alpha\vec{u}\cdot\nabla u)$
$\Delta_x F_\pi^a$	Zonal pressure working rate due to advection of the meridional velocity field	$\partial_x(p\alpha\vec{u}\cdot\nabla v)$
$\Delta_x F_k$	Zonal kinetic energy advective working rate	$-\alpha\,\partial_x(uK)$
$\Delta_y F_k$	Meridional kinetic energy advective working rate	$-\alpha\,\partial_y(vK)$
ΔF_π^β	Pressure working rate due to Coriolis acceleration	$\beta\frac{(p^2)_x}{2} \equiv \nabla\cdot(\beta y\vec{u}p)$
δf_π^t	Vertical pressure energy flux divergence due to time changes in density	$\partial_z(p\Gamma^2\sigma p_{zt})$
δf_π^a	Vertical pressure energy flux divergence due to horizontal advection of density	$\partial_z(p\alpha\Gamma^2\vec{u}\cdot\nabla\sigma p_z)$
$\Delta_y F_A$	Meridional A.G.E. advective working rate	$-\alpha\,\partial_y(vA)$
$\Delta_x F_A$	Zonal A.G.E. advective working rate	$-\alpha\,\partial_x(uA)$

Any nondivergent vector could be added to $\vec{\mathbf{F}}$ without changing (17a), an arbitrariness implied in any definition of energy flux. This vector contains the E-vector of Plumb (1985) but it is defined for the total flow variables and for an Eulerian system of reference. It contains advective fluxes and radiative fluxes in the form of pressure work done by ageostrophic fields, and it will be useful for the diagnosis of the propagation of energy in arbitrary open ocean regions.

Equation 17a can be written in terms of the dynamical vorticity (13c)

$$\frac{\partial}{\partial t}(K_0 + A_0) = +\nabla\cdot\left(\vec{\mathbf{u}}_0\alpha p_0\left(p_{0xx} + p_{0yy} + \Gamma^2(\sigma p_{0z})_z\right) + \beta y p_0\vec{\mathbf{u}}_0\right) + \nabla\cdot(p_0\nabla p_{0t}) + \partial_z\left(p_0\Gamma^2\sigma p_{0zt}\right) \tag{19}$$

with the identification,

$$\alpha\nabla\cdot(p_0\vec{\mathbf{u}}_0 q) = \Delta F_\kappa + \Delta F_A + \Delta F_\pi^a + \delta f_\pi^a \tag{20}$$

Equation 19 is equivalent to the quadratic energy invariant formulated directly from the vorticity dynamics, by multiplying eq. 13a by $-p_0$ and writing

$$-p_0\left[\partial_t\left[\nabla^2 p_0\right] + \Gamma^2\,\partial_t(\sigma p_{0z})_z\right] = +\alpha\,\nabla\cdot(\vec{\mathbf{u}}_0 p_0 q) + \beta p_{0x} p_0$$

which is discussed in Pedlosky (1979). On the other hand, our approach demonstrates the connection between the terms in the primitive energy equations (7a, b) and the form they assume in the quasigeostrophic regime.

4. SUMMARY EQUATIONS FOR ENERGY AND VORTICITY ANALYSIS—EVA

In the framework of quasigeostrophic dynamics many different phenomena occur characterized by different basic physical processes: wave propagation, instabilities, nonlinear interactions, horizontal and vertical cascades, turbulence, solitons, etc. The aim of this work is the interpretation of local dynamical mesoscale processes described by the dynamical vorticity equation (13) and energetically by eqs. 16 and 9. While the study of local vorticity balances can give quantitative information about the redistribution of vorticity within the flow, the energy analysis is helpful for the physical interpretation of the processes, for their classification in terms of local instabilities and for the elucidation of the transport mechanisms in open regions. It is necessary to study time series of maps of terms occurring in the equations for a long enough period to obtain unambiguous results in appropriately chosen subregions of the flow. The choice of space-time study domains is illustrated later in the paper.

Here we summarize the symbols, terms and equations that we will use in the examples of this paper and in future analyses of data sets and numerical model results. The vorticity equation is (13)

$$\partial_t q = \partial_t \nabla^2 p + \Gamma^2\,\partial_t(\sigma p_z)_z = -\alpha\,\nabla\cdot(\vec{\mathbf{u}}\nabla^2 p) - \alpha\Gamma^2\,\nabla\cdot(\vec{\mathbf{u}}(\sigma p_z)_z) - \beta p_x \tag{13a}$$

$$\dot{Q} = \dot{R} + \dot{T} = \Delta F_R + \Delta F_T + \Delta F_P \tag{13b}$$

with reference to Table III. The energy equations are (16a) and (9a)

$$\frac{\partial}{\partial t}K_0 = -\alpha\,\nabla\cdot(\vec{\mathbf{u}}_0 K_0) - \nabla\cdot\left(p_0\hat{k}\times\vec{\mathbf{u}}_{0t} + \alpha p_0\vec{\mathbf{u}}_0\cdot\nabla(\hat{k}\times\vec{\mathbf{u}}_0) - \beta y p_0\vec{\mathbf{u}}_0\right)$$
$$+\left(p_0\sigma\Gamma^2 p_{0zt} + p_0\alpha\Gamma^2\sigma\vec{\mathbf{u}}_0\cdot\nabla p_{0z}\right)_z + \delta_0 w_1 \tag{16a}$$

$$\dot{K} = \Delta F_k + \Delta F_\pi^t + \Delta F_\pi^a + \Delta F_\pi^\beta + \delta f_\pi^t + \delta f_\pi^a - b \tag{16b}$$

$$\frac{\partial}{\partial t}A = -\alpha\,\nabla\cdot(\vec{\mathbf{u}}A) - \delta w \tag{9a}$$

$$\dot{A} = \Delta F_A + b \tag{9b}$$

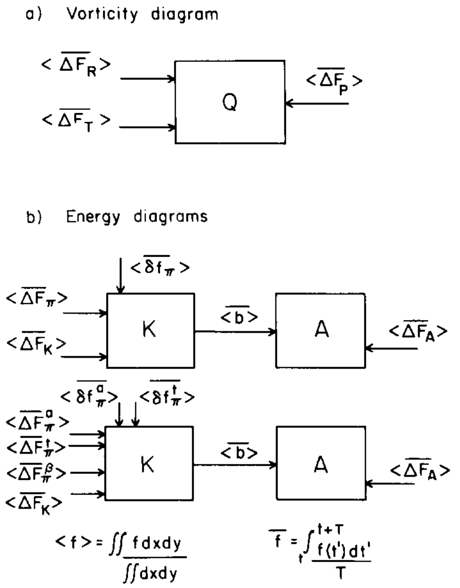

Fig. 1. (a) Vorticity diagram for integrated divergences of advective vorticity fluxes. (b) Energy diagram for integrated terms in the energy equations (16) and (9). The area integral is done in an arbitrary domain in the horizontal plane.

with reference to Tables II and IV. The non-dimensional parameters are found in Table I. Note that in the equations and tables of this section and henceforth we drop the subscripts 0 and 1 on the expanded field variables.

In our analyses we will present maps of the instantaneous vorticity tendencies in (13) and working rates in (16), (9). In Fig. 1 we define schematic vorticity and energy budget diagrams for the horizontal and time integral values of the terms in eqs. 13, 16 and 9. We construct the diagrams of Fig. 1 only after long enough time has passed for the arrows to be meaningful.

The Energy and Vorticity Analysis scheme summarized here, we refer to by the name EVA. This analysis scheme has been designed to be applied to any geostrophic pressure field, e.g., results of model runs, objective maps of oceanic data, etc.

The vorticity equation terms (13) are evaluated with finite elements in the horizontal and finite differences in vertical as in the model of Miller et al. (1983). The derivatives in the energy equations (16) and (9) are evaluated with a fourth order finite difference scheme in horizontal, the finite difference scheme of Miller et al. (1983) in vertical, and centered time differencing for the time rate of change of K and A. The code has been checked and validated using the results of the open ocean baroclinic quasigeostrophic model of Miller et al. (1983). The numerical schemes used for the energy equations have been found to give accurate ($\leq 1\%$) balances in the interior of the domain of integration. We neglect two points on each boundary because of the mismatch between the quasigeostrophic model and the energy equations numerical schemes.

5. THE BAROCLINIC ROSSBY WAVE

We use eqs. 16a and 9a to describe the energetic signature, in an Eulerian system of reference, of a horizontally propagating baroclinic Rossby wave. The streamfunction is

$$p = A(z)\cos(kx + ly - \omega t) \tag{21}$$

with $\omega = (-\beta k)/(k^2 + l^2 + \lambda^2)$, $\lambda^2 = D^2/R^2$. $A(z)$ is the vertical shape of the first internal baroclinic mode for a particular $N^2(z)$ and R is the first internal Rossby radius of deformation. Equation 21 is an exact solution of the vorticity equation (13) for rigid bottom and top boundary conditions ($w_1 = 0$ at $z = 0, -H$). We take $N^2(z)$ from the MODE-I region and choose for $A(z)$ the first baroclinic mode as illustrated in Miller et al. (1983).

The $\dot{K}$ and $\dot{A}$ equations for the wave solution (21) reduce to

$$\frac{\partial}{\partial t}K = \nabla \cdot (p\,\nabla p_t) + \nabla \cdot \left(\beta \frac{p^2 \hat{i}}{2}\right) + \partial_z(\sigma \Gamma^2 p p_{zt}) + p_z w$$

$$\dot{K} = \Delta F_\pi^t + \Delta F_\pi^\beta + \delta f_\pi^t - b$$

$$\frac{\partial A}{\partial t} = -p_z w$$

$$\dot{A} = b$$

The Rossby wave is a particular nonlinear solution of eq. 13, the one which makes $J(p, q) = 0$. Then from (20) $\Delta F_\pi^a = 0 = \Delta F_\kappa = \Delta F_A = \delta f_\pi^a$; there is no net work done by advective and nonlinear pressure work fluxes divergence meaning that there is no net growth of energy in the domain. We can already discriminate between the ΔF_κ, ΔF_A, δf_π^a, ΔF_π^a and ΔF_π^β, ΔF_π^t, δf_π^t: the latter are associated in an Eulerian system of reference with the Rossby wave radiative flux while the advective and nonlinear pressure work flux divergence are due to the interaction of the waves with a nonhomogeneous environment.

In Fig. 2 the terms in the right hand side of the kinetic energy equation are displayed. The terms show a symmetric wave pattern, high and lows alternating in the domain with equal amplitude in absolute value with a

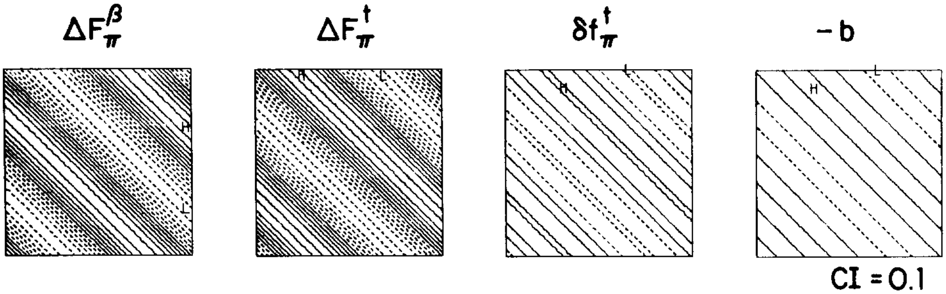

Fig. 2. Instantaneous maps of all the terms in eq. 16 at fixed z in the fluid for the Rossby wave solution (21). The abscissa of the pictures is in the zonal direction (x), the ordinate in the latitudinal (y).

periodicity of half the wavelength of the wave. The horizontal divergence of pressure work ($\Delta F_\pi^t + \Delta F_\pi^\beta$) is spatially anticorrelated with the buoyancy work term at all levels, i.e., whenever the buoyancy work converts locally $A(K)$ into $K(A)$, there is export (import) via horizontal pressure work flux divergence. This is the mechanism which maintains the horizontal transport of energy by baroclinic Rossby waves in the domain. It is associated with the linear part of the ageostrophic pressure work flux divergence: the wave has no net transport of energy in the domain via ΔF_κ or ΔF_A but it does work on the environment due to its ageostrophic motion. The δf_π^t contribution is also important but since $\int_{-H}^{0} \delta f_\pi^t \, dz = 0$ the phase of this term with respect to b and ΔF_π changes with depth.

In conclusion, the net horizontal kinetic energy transport by the wave is due to the correlation between p_0 and that part of $\vec{u}_1$ which corresponds to time rate of change of the geostrophic velocity and rotational effects due to β. This energy flux ($\vec{F}_\pi^t + \vec{F}_\pi^\beta$) is associated with the group velocity of the wave as opposed to the one defined in Longuet-Higgins (1964).

In terms of energy integrals, if we take any subdomain in Fig. 2 and we average in x, y and t for any integral number of *half* wave periods the net contribution from each of the terms in eqs. 16 and 9 is zero.

The case of an advected Rossby wave of the form

$$p = A(z) \cos(kx + ly - \omega t) - uy$$

where u is a zonally uniform flow, is similar to the case just described of a single Rossby wave. This time ΔF_κ, ΔF_A, δf_π^a, ΔF_π^a are different from zero but the instantaneous maps of the terms in (16) and (9) are still symmetric in the pattern of highs and lows. The time integral of all terms in eqs. 16 and 9, for any spatial subdomain average, now vanishes for any integer multiple of the wave period itself. This will be the case for any wave advected by a larger scale mean flow as we will see later.

6. THE BAROCLINICALLY UNSTABLE EADY WAVES

The aim is to describe the local energy dynamics of baroclinic flows unstable to infinitesimal disturbances. The local growth of mechanical energy density $(K + A)$ of the disturbance is associated with the conversion of available gravitational energy from the mean flow which is maintained constantly at the same level of energy. No feedback of energy to the mean flow is considered and the problem accurately represents only the initial growth of waves. Although the assumption of small amplitude perturbations growing on a larger scale mean flow is not applicable directly to many realistic geophysical fluid dynamics problems, this example is useful for comparative and interpretative purposes. In the past considerable attention has been paid to the study of the integrated energetics of the unstable Eady waves. Here we want to show the local transport/conversion of energy in the Eady waves for a subportion of the fluid which contains only a small part of the wave and to find the signature of the process.

The zonal mean flow $\bar{u}$ is uniform in y, varying linearly in z between two vertical boundaries and confined between two rigid walls at $y = \pm 1$ in a uniformly rotating system (Eady, 1949). We expand in the amplitude γ of the perturbation, i.e., $p = \bar{p} + \gamma p^{(1)} + \gamma^2 p^{(2)} + \cdots$ The vorticity equation for $p^{(1)}(x, y, z, t)$ is

$$(\partial_t + \bar{u}\,\partial_x)(\nabla^2 p^{(1)} + \Gamma^2 \sigma p^{(1)}_{zz}) = 0 \tag{22}$$

where $\sigma = 1$, $\Gamma^2 = 4$, $\bar{u} = -\bar{p}_y$, $\alpha = 1$. The boundary conditions are

$$\begin{aligned} &w_1^{(1)} = \partial_t p_z^{(1)} + \bar{u} p_{zx}^{(1)} - p_x^{(1)} = 0 \quad && \text{at } z = 0, 1 \\ &p_x^{(1)} = 0 && \text{at } y = \pm 1 \end{aligned} \tag{23}$$

The solution of eq. 22 is found in terms of normal modes of the form

$$p^{(1)} = B(z)\, e^{k c_i t} \cos ly \cos\left(kx + \alpha(z) - \frac{kt}{2} \right) \tag{24}$$

where

$$\alpha(z) = tg^{-1}\left[\frac{c_i \sinh \mu z}{\mu |c|^2 \cosh \mu z - \frac{1}{2} \sinh \mu z} \right]$$

$$B(z) = \sqrt{\left(\cosh \mu z - \frac{\sinh \mu z}{2\mu |c|^2} \right)^2 + \frac{c_i^2 \sinh^2 \mu z}{\mu^2 |c|^4}}$$

$$\mu^2 = \frac{(k^2 + l^2)}{\Gamma^2},$$

$$c = c_R + ic_i = \tfrac{1}{2} + \frac{i}{\mu} \sqrt{\left(\frac{\mu}{2} - \coth \frac{\mu}{2} \right)\left(\frac{\mu}{2} - \tanh \frac{\mu}{2} \right)}$$

and

$l = (n + 1/2)\pi, \quad n = 0, 1, \ldots$

The expansion of the relevant energy equations (16), (9) in γ is given in Appendix 1. We note that the contributions $K^{(1)}$, $A^{(1)}$ are not positive definite, and, in fact, that A8 and A9 could be obtained by multiplying (22) and the $0(\gamma)$ expansion of (12), respectively, by $\bar{p}$, $\bar{p}_z$. Note also that both sets $\dot{K}^{(1)}$, $\dot{A}^{(1)}$ and $\dot{K}^{(2)}$, $\dot{A}^{(2)}$ can be evaluated directly in terms of the first order growing perturbation solution eq. 24. The second order contribution governed by eqs. A10 and A11 are positive definite and contain the usual conversion terms from mean to perturbation energy.

We proceed to evaluate the $O(\gamma)$ eqs. A8 and A9 with (24). For both neutral and unstable solutions the instantaneous maps of each of the terms

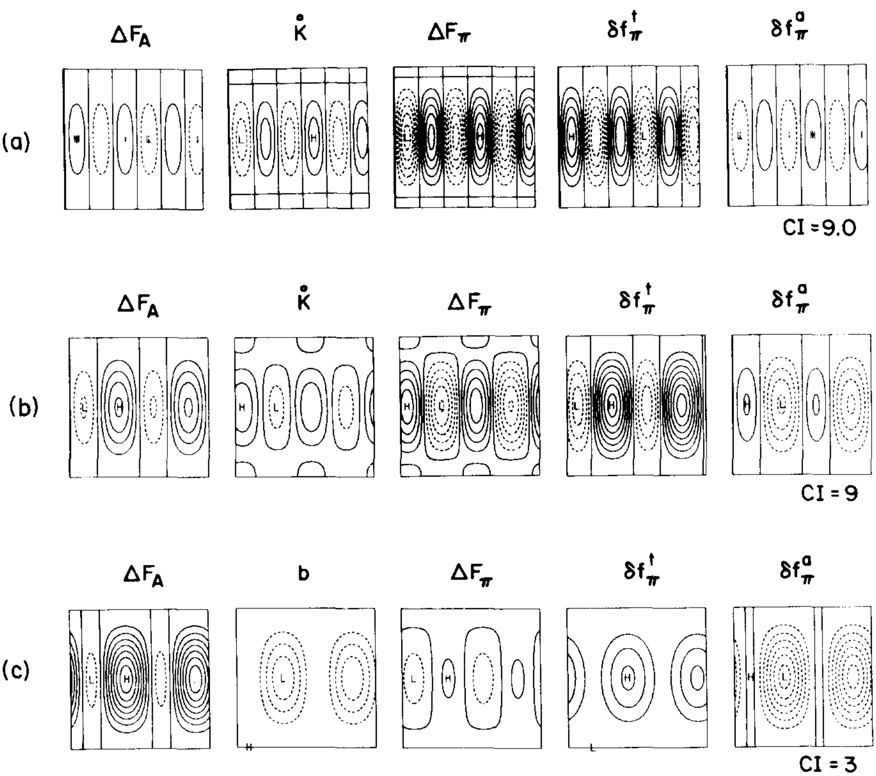

Fig. 3. (a) Instantaneous maps of terms in eqs. 25 and 26 for $t = 0.8$ (nondimensional) and $z = 0$. Neutral Eady wave case ($k = 4.5344$ and $l = \pi/2$). (b) Instantaneous maps of the terms in eqs. 25 and 26 for $z = 0$ and $k = \pi$, $l = \pi/2$: unstable Eady wave case. (c) Same as in (b) but at $z = 0.5$.

appear as simple alternating patterns of highs and lows with the same absolute value and equal areas over a wavelength. The pattern is not shown here because it is analogous to the structures of Fig. 3a, although this time the zonal periodicity is equal to the zonal wavelength of the wave and the meridional periodicity is half the meridional wavelength. A spatial average of the terms over a wavelength or a selected domain vanishes. For the neutral solution the average in time of the terms in eqs. A8 and A9 vanishes if the temporal interval is equal to the period of the propagating wave. At any point in the field the time series of each term in the unstable wave case is a simple growing wave form. Thus the integral from zero to T, as T steadily increases, fluctuates about zero. These properties occur in the $O(\gamma)$ balance for any growing normal mode, since each term is simply a product of two mean fields and a first order field. Thus the first order energetic processes are simply redistributions of energy with no conversion process signature. Instantaneously the stable and unstable wave pattern of the terms in eqs. A8 and A9 is symmetric, i.e., highs and lows occupy the same space and have equal magnitude in absolute value.

The signature of the local energy growth is contained in the $O(\gamma^2)$ balance of terms in eqs. A10 and A11. The $\dot{K}^{(2)}$ and $\dot{A}^{(2)}$ equations with $\bar{u}(z)$ only reduce to

$$\frac{\partial}{\partial t}K^{(2)} = -\bar{u}\,\partial_x K^{(2)} + \nabla\cdot\left(p^{(1)}\,\nabla p_t^{(1)}\right) + \nabla\cdot\left(p^{(1)}\bar{u}\,\partial_x\,\nabla p^{(1)}\right)$$
$$+\partial_z\left(\Gamma^2\sigma p^{(1)}p_{zt}^{(1)}\right) + \partial_z\left(\Gamma^2\sigma p^{(1)}\bar{u}p_{zx}^{(1)} + \Gamma^2\sigma p^{(1)}v^{(1)}\bar{p}_{zy}\right) + p_z^{(1)}w_1^{(1)} \tag{25}$$

$$\dot{K} = \Delta F_\kappa + \Delta F_\pi^t + \Delta F_\pi^a + O + \delta f_\pi^t + \delta f_\pi^a - b \tag{16b}$$

$$\frac{\partial}{\partial t}A^{(2)} = -\bar{u}\,\partial_x A^{(2)} - \Gamma^2\sigma p_z^{(1)}v^{(1)}\bar{p}_{zy} - p_z^{(1)}w_1^{(1)} \tag{26}$$

$$\dot{A} = \Delta_x F_A + \Delta_y F_A + b \tag{9b}$$

where

$$K^{(2)} = \frac{u^{(1)^2} + v^{(1)^2}}{2} \text{ and } A^{(2)} = \frac{\Gamma^2\sigma\left(p_z^{(1)}\right)^2}{2}$$

As indicated in (25) and (26) the advective (ΔF_κ, ΔF_A) and nonlinear pressure work (δf_π^a, ΔF_π^a) flux divergences involve interactions of the wave fields $p^{(1)}$, $v^{(1)}$, $u^{(1)}$ with the mean flow. Furthermore only the $\Delta_y F_A$ and part of δf_π^a contain the interaction of the wave with the vertical shear of the flow, which is the seat of the conversion of the mean flow energy to wave energy. To this order in the γ expansion the other terms ΔF_π^t, δf_π^t are similar to the free Rossby wave radiative flux divergences.

Figure 3a shows some of the terms in eqs. 25 and 26 for a neutrally stable wave with $k = 4.5344$, $l = \pi/2$. This neutral solution shows terms similar to the baroclinic Rossby wave solution of before, high and lows alternating in the field with the same absolute value and with a periodicity of half the zonal wavelength of the wave. The interpretation is exactly as in section 5 for the nonadvected wave.

The case of the growing wave is shown in Fig. 3b, c at two different depths in the fluid. The presence of instability is indicated by asymmetric patterns (i.e., the uneven spacing and unequal amplitudes of the highs and lows) of the terms δf_π^t, δf_π^a, b, ΔF_π^t and ΔF_A. The source of energy for the disturbance is the available gravitational energy of the mean flow. $\Delta_y F_A$ represents the rate of doing work by the wave 'Reynolds heat flux', $p_x^{(1)} p_z^{(1)}$, against the meridional gradient of mean temperature $\bar{p}_{zy}$. ΔF_A is asymmetric at all levels and positive definite in the sense that the absolute value of the highs is bigger than the lows: it is the well known 'source' term for the unstable waves.

At the steering level (Fig. 3c) the buoyancy work is negative definite, i.e., is converting $A^{(2)}$ into $K^{(2)}$; this represents the internal conversion process which allows the kinetic energy of the wave to grow at the expense of its available gravitational energy. The latter is growing at the expense of the mean flow available gravitational energy. At the vertical boundaries (Fig. 3b) the buoyancy work is equal to zero since $w_1^{(1)} = 0$.

The vertical pressure working rate δf_π is the sum of its components $\delta f_\pi^{t,a}$ shown in Fig. 3. The vertically integrated δf_π contribution is equal to zero because of the boundary conditions (23) and its symmetry about the steering level. Thus δf_π changes sign between the vertical walls and the steering level. In particular between $z = 0$ and $z = 0.2$, δf_π imports energy while between $z = 0.2$ and $z = 0.5$ it exports it. The levels close to the vertical boundaries receive kinetic energy by vertical pressure work energy flux divergence from the interior of the fluid where the conversion via b is strongest.

Componentwise, δf_π^t is positive, and δf_π^a is negative definite. δf_π^a, which contains the pressure work energy flux $p^{(1)} v^{(1)} \sigma \bar{p}_{zy}$, represents the rate of energy lost by the wave which at finite amplitude decreases the shear in the mean flow. It is interesting to point out that δf_π^a and $\Delta_y F_A$ contain cross-correlations of the perturbation fields weighted by the mean flow shear which make the patterns asymmetric. If we compare δf_π^a and ΔF_A at the steering and boundary level, we see that the maximum local negative value of δf_π^a and positive value of ΔF_A is also at the boundaries. At *every level* the wave radiation field gives a net (in a negative definite sense) divergence of energy fluxes due to δf_π^a. Finally all the other terms, ΔF_π^a, ΔF_κ, $\Delta_x F_A$ only

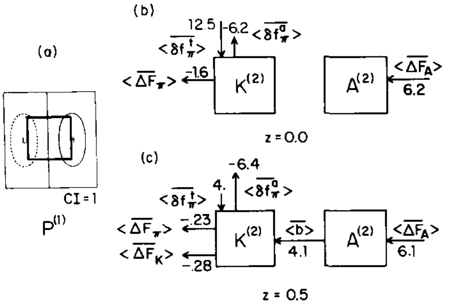

Fig. 4. Energy diagram for unstable Eady case. (a) Domain of integration superimposed on the instantaneous $p^{(1)}$ field, (b) energy diagram at $z = 0$, (c) energy diagram at $z = 0.5$.

involve advections by the mean flow $\bar{u}$ which yield symmetric patterns. ΔF_π is also asymmetric due to ΔF_π^t (not shown here); this is due to local growth of radiative transport of energy by the growing wave but does not involve interactions with the mean flow.

We have taken horizontal domain integrals in a subportion of the flow field shown in Fig. 3 for the terms in eqs. 25 and 26 in the unstable case. We have then calculated the horizontal and time averaged $\langle\overline{K^{(2)}}\rangle$ and $\langle\overline{A^{(2)}}\rangle$ balances in this subdomain for a time integral corresponding to half of the period of the neutral waves. The values are presented in Fig. 4. As noted above, the $\langle\overline{\delta f_\pi^a}\rangle$ decreases the kinetic energy of the perturbation while $\langle\overline{\delta f_\pi^t}\rangle$ increases it; the $\langle\overline{\Delta F_\pi}\rangle$, $\langle\overline{\Delta F_\kappa}\rangle$ always export K, and at the steering level $\langle\overline{-b}\rangle$ has its maximum positive value. $\langle\overline{\Delta F_A}\rangle$ is always positive. $\langle\overline{\delta f_\pi}\rangle$ changes sign between the boundary and the steering level but $\langle\overline{\delta f_\pi^a}\rangle$ and $\langle\overline{\delta f_\pi^t}\rangle$ always have the same sign since the wave energy is growing everywhere and work is done against the horizontal mean gradient of temperature.

We are interested in capturing the local signatures of the instability not only in the $O(\gamma^2)$ equations but in a more realistic situation where both $O(\gamma)$ and $O(\gamma^2)$ contributions are not easily separated. We have then added eqs. 25 and 26 multiplied by γ^2 to the $O(\gamma)$ eqs. A8 and A9. The fields produced by this combined balance are shown in Fig. 5 for the case of the unstable wave with $\gamma = 0.01$ at twice the e-folding time (total amplitude ~ 0.1). The fields show more complicated structures than in Fig. 3 but the asymmetries in the pattern are present in the same terms. More importantly the terms conserve the positive or negative definiteness as before. The integral in space and time of the terms in Fig. 5 thus have exactly the same direction of energy transport/conversion as in Fig. 4. The signature of the baroclinically unstable process for a realistic oceanic case as characterized by this study are: in the presence of growth of A and K (1) growing

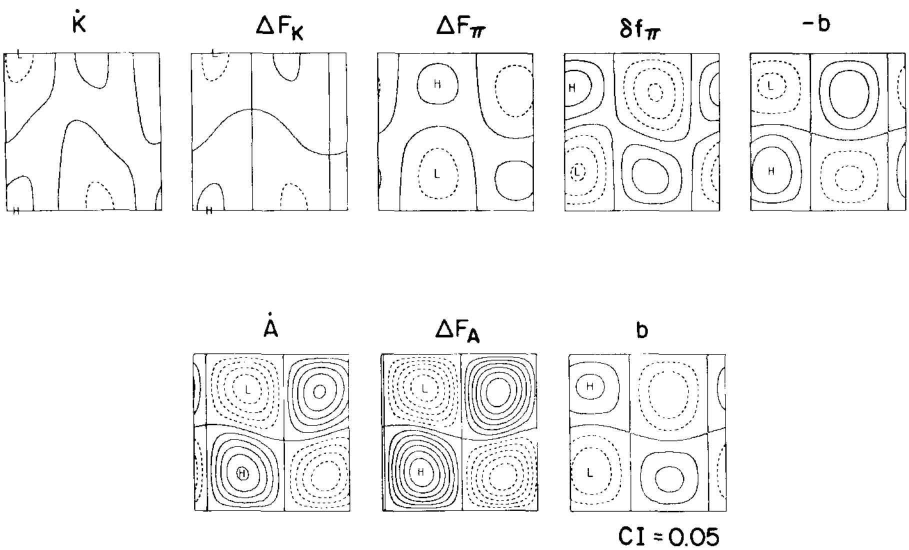

Fig. 5. Instantaneous maps for the unstable Eady case: $O(\gamma)+O(\gamma^2)$ balance, $z = 0.5$.

asymmetries in ΔF_A, b, δf_π and ΔF_π^l; (2) the positive (negative) definiteness of each of these terms; and (3) integrated energy diagram as in Fig. 4 for an event separable from a space–time background situation.

7. THE BAROTROPIC INSTABILITY PROBLEM

In this section we illustrate the local transport/conversion energetics and signatures for the case that the energy source for the growing waves lies in the kinetic energy of the mean flow and the process involves the mean horizontal shear. The analytical example chosen is mathematically very simple and depth independent. The barotropic mean flow is $\bar{u} = y$ between $y = 0,1$ and constant outside this region: at $y = 0,1$ we have then a jump in $\bar{u}_y$ which results in a source of energy for the waves. This is essentially the example presented by Gill (1982).

The fields ϕ: p, u, v, w are expanded in the small amplitude γ of the perturbation and the $O(\gamma)$ perturbation is assumed to be everywhere a zonally propagating normal mode. The vorticity equation to the first order in γ is

$$[\partial_t + \bar{u}\,\partial_x]\ \nabla^2 p^{(1)} = 0 \tag{27}$$

where α is taken to be 1.

At $y = 0,1$ the continuity of the geostrophic normal velocity v_0 is imposed and the solution outside the meridional interval [0,1] is assumed to decay exponentially. Also at $y = 0{,}1$ we impose the continuity of the $O(\gamma)$ ageostrophic meridional velocity v_1, i.e.

$$v^{(1)} = -[\partial_t + \bar{u}\,\partial_x]\, p_y^{(1)} + p_x^{(1)} \tag{28}$$

The solution in the meridional interval [0,1] is found to be of the form

$$p^{(1)} = \mathrm{e}^{kc_i t}\left[\alpha(y)\cos\left(kx - \frac{kt}{2}\right) + \beta(y)\sin\left(kx - \frac{kt}{2}\right)\right] \tag{29}$$

where

$$c = c_R + ic_i,\ c_R = \tfrac{1}{2}$$

$$\alpha(y) = \left[\frac{\dfrac{1}{4} - \dfrac{1}{2k} + c_i^2}{\left(\dfrac{1}{2} - \dfrac{1}{k}\right)^2 + c_i^2}\right]\cosh ky + \sinh ky$$

$$\beta(y) = \frac{c_i \cosh ky}{k\left[\left(\dfrac{1}{2} - \dfrac{1}{k}\right)^2 + c_i^2\right]}$$

$$c_i = \sqrt{\frac{\mathrm{e}^{-2k}}{4k^2} - \left(\frac{1}{2} - \frac{1}{2k}\right)}$$

c_i is greater than zero if $k < k_c = 1.2785$ and as in the Eady problem we have a short wave cut-off.

In Appendix 1 the relevant terms in the $O(\gamma)$ and $O(\gamma^2)$ equations are displayed and in particular the $O(\gamma^2)$ balance for $\bar{u} = y$ only, reduces eq. A10 to

$$\frac{\partial}{\partial t}K^{(2)} = -\bar{u}\,\partial_x K^{(1)} - u^{(1)}v^{(1)}\bar{u}_y + \nabla\cdot\left(p^{(1)}\,\nabla p_t^{(1)}\right)$$
$$+\nabla\cdot\left(p^{(1)}\bar{u}\,\partial_x\nabla p^{(1)} + p^{(1)}v^{(1)}\bar{p}_{yy}\hat{j}\right) \tag{30}$$

$$\dot{K} = \Delta_x F_\kappa + \Delta_y F_\kappa + \Delta F_\pi^t + \Delta F_\pi^a + 0 + 0 + 0 \tag{16b}$$

For stable and unstable waves the maps of the $O(\gamma)$ terms (eq. A8) show high and lows alternating in the field with the same absolute values, a symmetric pattern. The interpretation is analogous to the $O(\gamma)$ equation discussion of section 6. The $O(\gamma^2)$ equation again contains the 'source' terms for the instability or equivalently for the asymmetries in the flux divergence terms.

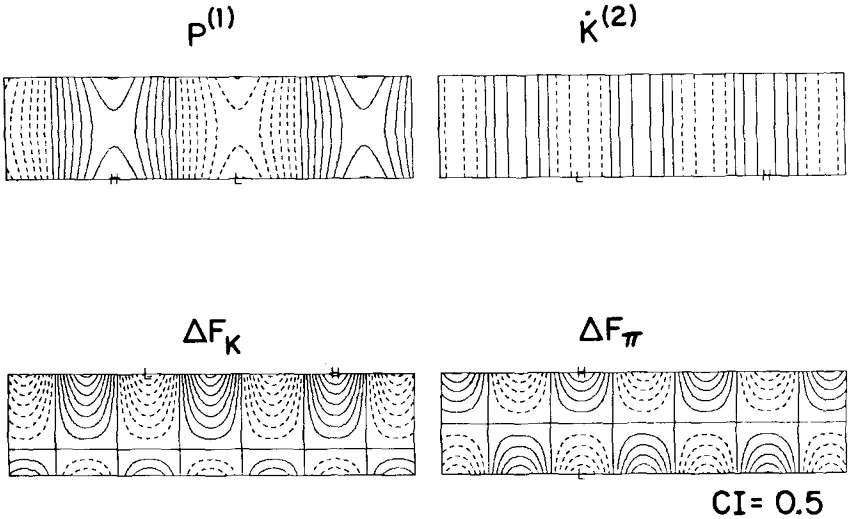

Fig. 6. Instantaneous maps of terms in eq. 30 for the stable barotropic wave, $k = 1.2785$, $t = 2$.

Figures 6 and 7 show some of the terms in eq. 30 for the fastest growing wave ($k = 0.7968$) and the neutrally stable wave ($k = 1.2785$). As before, the neutral case terms are perfectly symmetrical and the time integral over a multiple of half a wave period is zero. The unstable case (Fig. 7) is characterized by asymmetries in values of highs and lows. Only $\Delta_x F_\kappa$, $\Delta_x F_\pi^t$ and $\Delta_x F_\pi^a$ remain symmetric. The $\Delta_y F_\kappa$ term (which in the barotropic case is physically analogous to the 'source' term $\Delta_y F_A$ in the baroclinic instability case) contains the northward momentum flux due to the perturbation, $v^{(1)}u^{(1)}$. The only terms containing the interaction of the perturbation with the horizontal shear of the mean flow are $\Delta_y F_\kappa$ and part of ΔF_π^a. This time ΔF_π^a contains the pressure work flux by the perturbation $p^{(1)}v^{(1)}$ against the mean horizontal shear field $\bar{u}_y$. As expected both ΔF_π^a and $\Delta_y F_\kappa$ are larger in absolute value at $y = 0, 1$ where $\bar{q}_y$ changes sign.

We have taken the space–time integral of the terms in eq. 30 in different subdomains. The energy diagrams are shown in Fig. 8 for two different regions of integration, and for the time integral from zero to $T = \pi/kc_R$ as before. Here $\langle\overline{\Delta F_\pi^t}\rangle$ and $\langle\overline{\Delta F_\kappa}\rangle$ are positive everywhere. $\langle\overline{\Delta F_\pi^a}\rangle$ is negative since pressure work is done by the perturbation against the mean meridional gradient of $\bar{u}$; i.e., kinetic energy is lost by the perturbation working to decrease the shear in the mean flow. $\langle\overline{\Delta F_\pi}\rangle$ changes sign between the boundaries and the center of the domain since there is no energy flux in or out of the interval [0,1] but $\langle\overline{\Delta F_\pi^t}\rangle$ and $\langle\overline{\Delta F_\pi^a}\rangle$ have the same sign every-

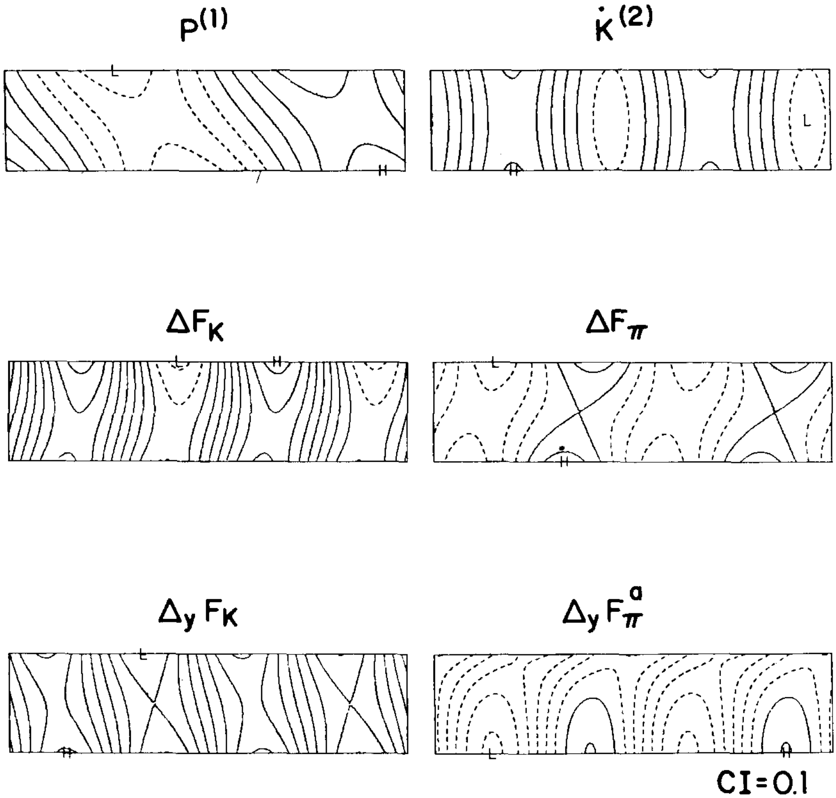

Fig. 7. Instantaneous maps of terms in eq. 30 for the unstable barotropic wave, $k = 0.7968$, $t = 2.0$.

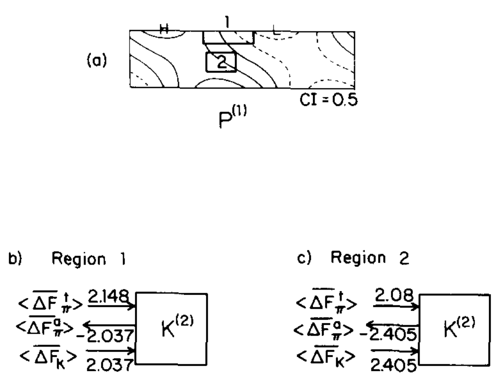

Fig. 8. Energy diagram for the unstable barotropic wave case. (a) different Horizontal domain of integration superimposed on the instantaneous $p^{(1)}$ field, (b) energy diagram for region 1, (c) energy diagram for region 2.

where. $\langle \overline{\Delta F_\kappa} \rangle$ and $\langle \overline{\Delta F_\pi^a} \rangle$ are equal in magnitude and opposite in sign since the total vorticity of the wave is zero (see eq. 20).

The $O(\gamma) + O(\gamma^2)$ balance (not shown here) presents the asymmetries in the same divergence terms of the $O(\gamma^2)$ balance. The positive (negative) definiteness of ΔF_κ, $\Delta F_\pi^t(\Delta F_\pi^a)$ persist also in this more realistic situation.

In conclusion barotropic instability is characterized by the growth of asymmetries in ΔF_κ, ΔF_π^a and ΔF_π^t terms with ΔF_κ, ΔF_π^t positive and ΔF_π^a negative definite.

8. DATA ANALYSIS

In this section we describe the analysis and the interpretation of a striking eddy merger event (Robinson et al., 1985a) revealed by the dynamical assimilation of oceanic data in the Harvard open ocean baroclinic quasigeostrophic model (Miller et al., 1983). The methodology of approach to dynamical forecasting and interpolation in the ocean is explained in general in Robinson and Leslie (1985) and in detail in Robinson et al. (1986b) (hereafter referred to as RCPM), in the context of the study of this particular forecast experiment in the California Current system. We believe the process involved to be a finite amplitude barotropic instability of a baroclinic flow. The data set and detailed physical analyses are presented in RCPM. Here we illustrate the deduction of physical process by subjecting quasigeostrophically filtered data to EVA, in the context of our derivations and prior examples.

The method consists of initializing the six level quasigeostrophic model with objectively analyzed data and integrating forward, updating the streamfunction p and the vorticity q at the boundaries as described below. This results in a spatially and temporally continuous model data set of quasigeostrophic pressure fields fully adjusted by the model to its internal dynamics. The local energy and vorticity budgets are evaluated on this dynamically interpolated data set; the advantage of this approach resides

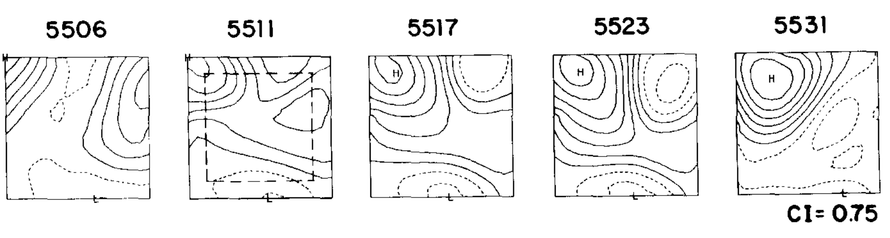

Fig. 9. Streamfunction maps for the forecast experiment starting at Julian day 5506, ending at Julian day 5534. Model level 2 at 150 m. The inner dashed box indicates the EVA domain.

both in the ability to relate with real data processes in the ocean and in allowing the test of dynamical assumptions contrasting the forecast fields with the measurements. In Fig. 9 the streamfunction of a 28 day forecast experiment is presented for a (150 km)^2 domain. The dynamical evolution of the streamfunction shows that two anticyclonic eddies merge during the first week, followed by a phase of expansion during the following 10 days and a subsequent phase of relaxation which leaves a single warm core eddy. Three 'quasisynoptic' data sets were available centered at days 0, 14, and 28. The *forecast experiment* uses day 0 for initialization, and only the boundary strip data of days 14 and 28 for boundary condition updating (with *a posteriori* linear interpolation). The interior data of days 14 and 28 were reserved for verifications which were very good (see RCPM).

Maps of the terms in the vorticity equation (13) are presented in Fig. 10. (Note that the EVA domain is stripped of the outer 20 km of the streamfunction maps domain so that boundary effects in EVA are physical.) At

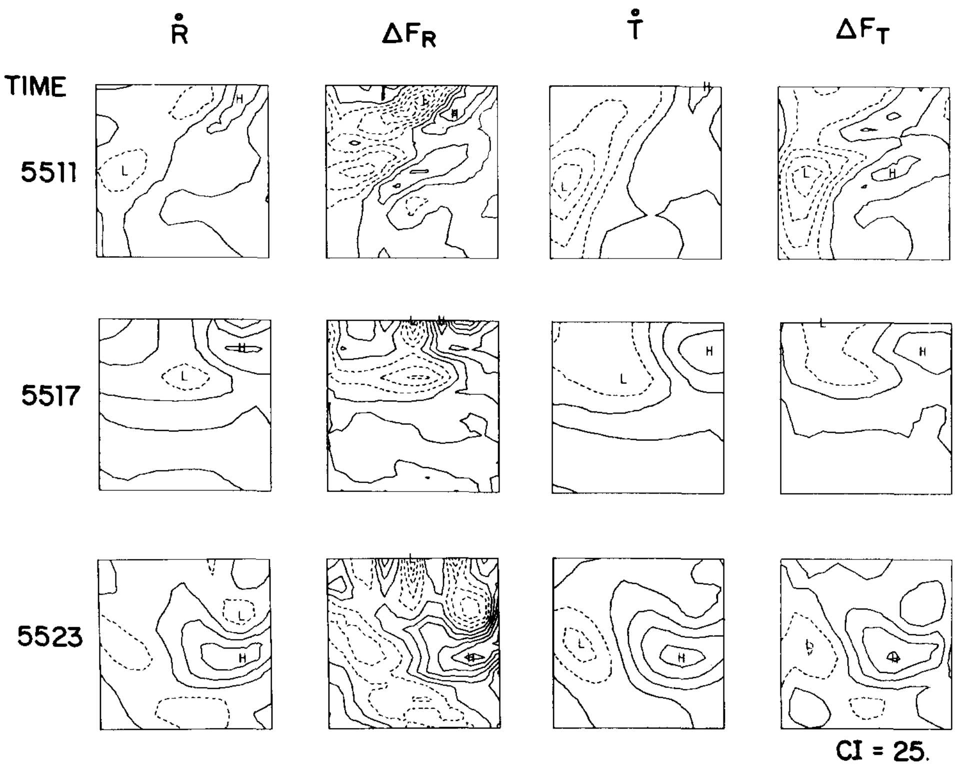

Fig. 10. Vorticity terms in eq. 13 at different times during the forecast experiment. Model level 2 (150 m).

this level (150 m), ΔF_R and ΔF_T are comparable during the first 5 days. In the 'neck' between the two eddies ΔF_R is the major contribution balanced by all other terms including a contribution (not shown) from a dissipative-like effect due to the filtering of vorticity (RCPM). In the following 10 days ΔF_R becomes dominant over the vortex stretching term. At 400 m depth (not shown here), the divergence of advective fluxes of relative vorticity is always dominant and the forecast shows that the merging occurs more rapidly than at any other level in the fluid. At the end of the expansion phase ΔF_R and ΔF_T are comparable (ΔF_R at somewhat smaller scales) and all the four terms contribute to the balance.

The energy analysis of the forecast experiment is shown in Figs. 11 and 12. The kinetic energy dynamics are dominated during the merger phase by a local decrease of kinetic energy in the northern eddy via both $\Delta_x F_\pi^a$ and $\Delta_x F_\kappa$ (not shown) but with a dominant contribution by $\Delta_x F_\pi^a$. Energy is imported into the domain mainly by $\Delta_y F_\pi^a$ which shows a strong convergence of radiative fluxes at the border of the northwestern eddy. At the same time $\Delta_x F_\kappa$ and $\Delta_x F_\pi^a$ grow locally in absolute value to almost balance the

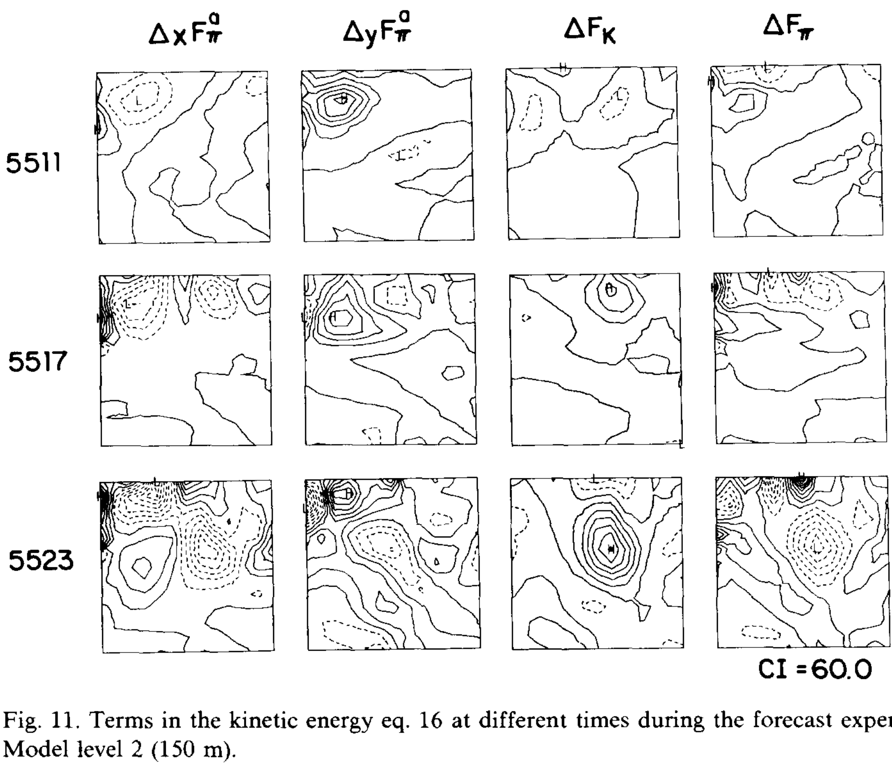

Fig. 11. Terms in the kinetic energy eq. 16 at different times during the forecast experiment. Model level 2 (150 m).

contribution from $\Delta_y F_\pi^a$ producing a divergence of energy fluxes in the same area. All the other terms in the kinetic energy equation are negligible at this level. During the expansion phase the horizontal divergence terms still dominate the evolution of the flow field; ΔF_κ now plays a major role. $\Delta_x F_\pi^a$ and $\Delta_y F_\pi^a$ change rapidly in time and contain somewhat smaller scales than in the first phase. ΔF_κ is positive and ΔF_π becomes negative such that it almost balances the contribution of ΔF_κ locally; this pattern is reminiscent of the barotropic instability case of section 7. Here, however, the asymmetries in ΔF_π^a and ΔF_κ grow a different rates. We interpret these behaviors during the expansion and merger phases as a sign of a local nonlinear energy conversion between different horizontal wavenumbers in the flow. A subsequent production of local divergence of energy fluxes decreases the shear in the area of interaction of the two eddies. During the relaxation phase there is a relatively simple balance between ΔF_π and ΔF_κ.

Although it is not important quantitatively to the $\dot{K}$ balance, an imbalance among the terms discussed here produced a conversion of K to A via b during the merger and expansion phases. The available gravitational energy equation maps (Fig. 12) show that A is increasing in the northern eddy. The

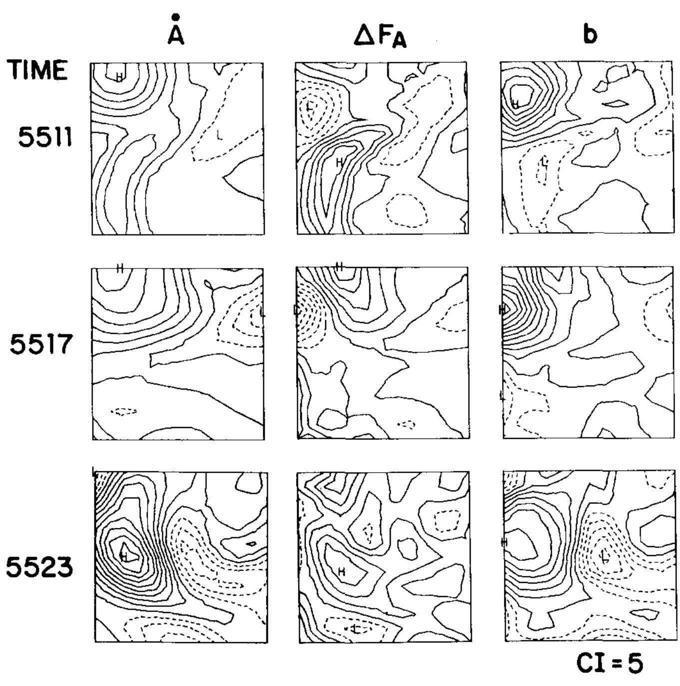

Fig. 12. Terms in the available gravitational energy equation (9) at different times during the forecast experiment. Model level 2 (150 m).

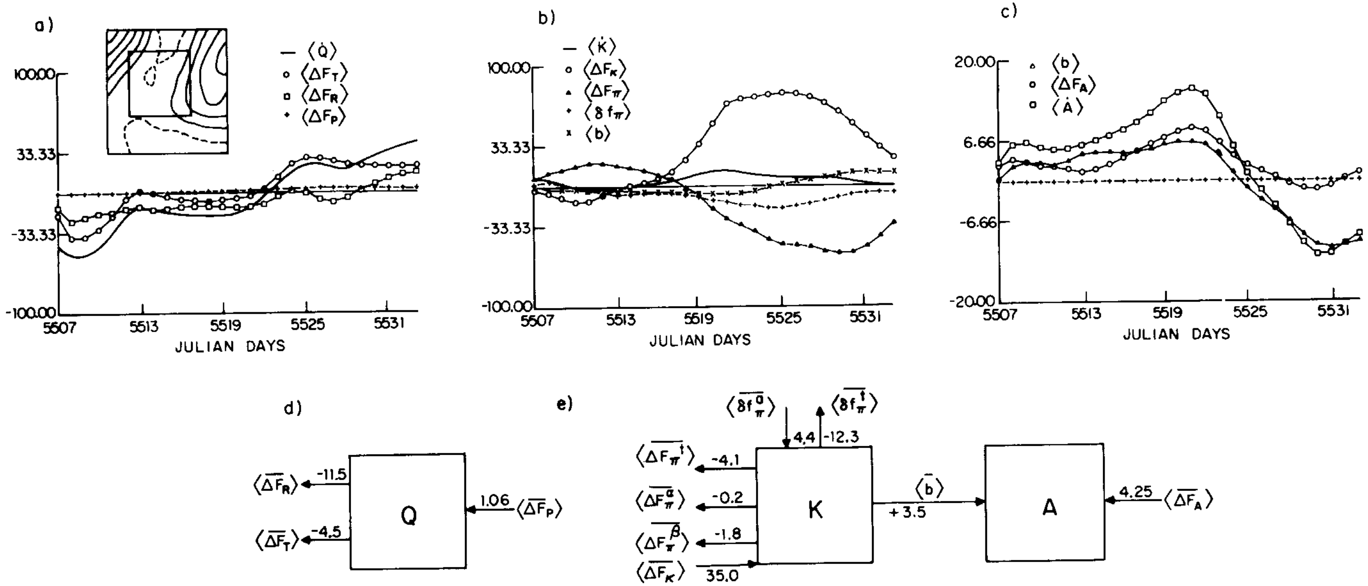

Fig. 13. Energy and vorticity diagrams for the forecast experiment (reproduced from RCPM). The inner domain used for averaging is shown in the upper left. (a) time rate of change of Q and divergences of the vorticity fluxes, (b) time rate of change of K, divergences of the kinetic energy fluxes and the negative of the buoyancy work, (c) the time rate of change, advective fluxes of A and buoyancy work, (d), (e) vorticity and energy diagrams. Arrows show the direction of the fluxes.

ΔF_A term is smaller than b during the merger phase in the region of interaction of the two eddies. During the relaxation phase ΔF_A and b become comparable and show an enhanced wave-like behavior.

In Fig. 13 the energy and vorticity diagrams for the forecast experiment are shown. The horizontal area integral is done in the region of original contact of the eddies. The time series a, b, c show clearly the three phases. The vorticity balances (Fig. 13a) show that during the merger phase the major contribution is given by $\langle \Delta F_R \rangle$ and the most noticeable change is the vanishing of $\langle \Delta F_T \rangle$. In the expansion phase $\langle \Delta F_R \rangle$ continues slowly to increase. During the relaxation phase, $\langle \Delta F_R \rangle$, $\langle \Delta F_T \rangle$ oscillate and change sign and $\langle \Delta F_T \rangle$ becomes the dominant contribution. Process-wise, the merger and expansion phases are lumped together because they show analogous local and integrated vorticity balances. In the $\dot{K}$ time series (Fig. 13b) the merger and expansion phases show remarkable changes in $\langle \Delta F_\kappa \rangle$ and $\langle \Delta F_\pi \rangle$. The onset of the expansion phase is indicated by the dramatic increase of $\langle \Delta F_\kappa \rangle$ and the sign change of $\langle \Delta F_\pi \rangle$. During the merger and expansion phases, $\langle b \rangle$ decreases the kinetic energy of the system and $\langle \delta f_\pi \rangle$ exports energy vertically. Towards the end of the relaxation phase all the contributions to the $\dot{K}$ balance are diminishing in absolute values. In the $\dot{A}$ balance (Fig. 13c) the maximum rates occur during the expansion phase which ends with a sign change of all the contributing terms.

The time integrals of the terms in the time series of Fig. 13 have been taken starting from the initial time until 20 days later, at the end of the expansion phase. The relaxation phase has been omitted because we think that it is a dynamically distinct process, as discussed before. The diagram shows that the $\langle \overline{\Delta F_\kappa} \rangle$ and $\langle \overline{\Delta F_\pi^a} \rangle$ components are opposite in sign in a manner consistent with the barotropic instability case of section 7. $\langle \bar{b} \rangle$ is positive and large in the interaction area of the eddies, comparable with $\langle \overline{\Delta F_A} \rangle$. At level 3 (not shown here) the contribution by $\langle \overline{\Delta F_A} \rangle$ is smaller than $\langle \bar{b} \rangle$ and the whole process of merging is faster. $\langle \overline{\delta f_\pi^I} \rangle$ and $\langle \overline{\Delta F_\pi^I} \rangle$ both diverge energy out of the interaction area of the two eddies.

The energy diagram supports the interpretation of the divergence maps: kinetic energy is redistributed horizontally by ΔF_π^a and ΔF_κ to larger horizontal scales and is converted to gravitational energy by buoyancy work. It is interesting to conjecture that this might be a generalizable characterization of ocean eddy merging processes.

9. DISCUSSION AND CONCLUSIONS

In this paper we develop and illustrate a method for studying physical processes in local, open domains of a fluid governed by quasigeostrophic dynamics. The physical diagnostics are chosen to be energy and vorticity balance analyses (EVA). The overall objective is to contribute to the dynamical analysis of real oceanic data and of data output from numerical models. Intensive data sets suitable for such dynamical analysis are limited in extent, and the dynamics of EGCM's is definitely spatially inhomogeneous. Thus open regional analysis is required. Important studies over the last few years have established the relevance of quasigeostrophic dynamics for many oceanic synoptic/mesoscale phenomena. Thus a consistent and comprehensive energy diagnostics for quasigeostrophic flows and relateable to more general flows is necessary and timely.

In this study we: (1) derive a consistent and useful statement of geostrophic energetics evaluated in terms of the quasigeostrophic pressure; (2) identify the ageostrophic origin of energy flux divergences; (3) relate the quasigeostrophic terms to their more general forms; (4) characterize some signatures of wave, instability, nonlinear interaction and conversion processes; and (5) illustrate the method of EVA applied to real data after quasigeostrophic filtering via numerical model interpolation. The EVA equations are summarized, all symbols are defined, and the combined use of time series of maps, appropriately chosen space and time integrals, and schematic diagrams is described in section 4. The signature of wave, baroclinic, and barotropic instability processes are summarized in the final paragraphs of each of sections 5, 6 and 7, respectively. Importantly, growing wave instabilities are characterized by asymmetric patterns in maps of terms of the energy equations (unequal areas for, and unequal amplitudes of, highs and lows). Our results indicate: for barotropic instability processes, positive definite ΔF_κ, b and negative definite ΔF_π^a; for baroclinic instability processes, positive definite ΔF_A, δf_π^t and negative definite ΔF_κ, ΔF_π, δf_π^a, b.

Theory, modeling, experimental and observational data acquisition and analysis interact importantly in modern oceanography. The direct inference of a local nonlinear physical process from data via novel methodology should be of increasing importance as data assimilation and large scale modeling advances. In addition to the California Current region we are utilizing EVA in the POLYMODE region and the Gulf-Stream system, and find it a useful tool. Our work in progress includes the extension to enstrophy analysis and the use of EVA on shipboard computers to guide real time evolution of synoptic/dynamical experiments.

ACKNOWLEDGMENTS

It is a pleasure to express our gratitude to Leonard Walstad, Prof. Brian Farrell and Antonio Navarra for interesting and helpful discussions. We also thank Dr. James A. Carton and Prof. Nick Fofonoff for critical comments and Chris Mullaney for careful typing of the paper. This research was supported by the Office of Naval Research under Contract N00014-84-0461 to Harvard University.

APPENDIX 1

Expansion of the energetics for instability studies

All fields ϕ_i: u_0, v_0, w_1, p_0 are expanded in the amplitude, γ, of the perturbation as

$$\phi_i = \phi_i^{(0)} + \gamma\phi_i^{(1)} + \gamma^2\phi_i^{(2)} + \cdots \tag{A1}$$

and $w_1^{(0)} = v_0^{(0)} = 0$, $u_0^{(0)} = \bar{u}(z, y)$, $p_0^{(0)} = \bar{p}(z, y)$. Here we take also $\beta = 0$. We now expand eqs. 16 and 9. The zeroth order expansion of eqs. 16 and 9 is identically equal to zero since the energy of the mean flow is not changed. To order γ^2 the terms in eqs. 16a and 9a result

$$\dot{K} = \Delta F_\kappa + \Delta F_\pi^t + \Delta F_\pi^a + \delta f_\pi^t + \delta f_\pi^a - b \tag{A2}$$

$$\dot{K} = \gamma\left(\partial_t(u^{(1)}\bar{u})\right) + \gamma^2\left(\partial_t\left(\frac{u^{(1)^2} + v^{(1)^2}}{2}\right) + \partial_t(u^{(2)}\bar{u})\right)$$

$$\Delta F_\kappa = -\gamma\left(\alpha\bar{u}\;\partial_x(u^{(1)}\bar{u}) + \alpha\vec{\mathbf{u}}^{(1)}\cdot\nabla\left(\frac{\bar{u}^2}{2}\right)\right) - \gamma^2\left(\alpha\bar{u}\;\partial_x\left(\frac{u^{(1)^2} + v^{(1)^2}}{2}\right)\right.$$
$$\left. + \alpha\bar{u}\;\partial_x(u^{(2)}\bar{u}) + \alpha\vec{\mathbf{u}}^{(1)}\cdot\nabla(u^{(1)}\bar{u}) + \alpha\vec{\mathbf{u}}^{(2)}\cdot\nabla\left(\frac{\bar{u}^2}{2}\right)\right)$$

$$\Delta F_\pi^t = \gamma\left(\nabla\cdot\left(\bar{p}\,\nabla p_t^{(1)}\right)\right) + \gamma^2\left(\nabla\cdot\left(\bar{p}\,\nabla p_t^{(2)}\right) + \nabla\cdot\left(p^{(1)}\,\nabla p_t^{(1)}\right)\right)$$

$$\Delta F_\pi^a = \gamma\left(\nabla\cdot\left(\bar{p}\alpha\bar{u}\;\partial_x\,\nabla p^{(1)}\right) + \nabla\cdot\left(\bar{p}\alpha\vec{\mathbf{u}}^{(1)}\cdot\nabla\nabla\bar{p}\right)\right)$$
$$+\gamma^2\left(\nabla\cdot\left(\bar{p}\alpha\bar{u}\;\partial_x\,\nabla p^{(2)}\right) + \nabla\cdot\left(\bar{p}\alpha\vec{\mathbf{u}}^{(1)}\cdot\nabla\nabla p^{(1)}\right) + \partial_y\left(\bar{p}\alpha v^{(2)}\bar{p}_{yy}\right)\right.$$
$$\left. + \nabla\cdot\left(p^{(1)}\alpha\bar{u}\;\partial_x\,\nabla p^{(1)}\right) + \partial_y\left(p^{(1)}\alpha v^{(1)}\bar{p}_{yy}\right)\right)$$

$$\delta f_\pi^t = \gamma\left(\partial_z\left(\sigma\Gamma^2\bar{p}p_{zt}^{(1)}\right)\right) + \gamma^2\left(\partial_z\left(\sigma\Gamma^2\bar{p}p_{zt}^{(2)} + \sigma\Gamma^2 p^{(1)}p_{zt}^{(1)}\right)\right)$$

$$\delta f_\pi^a = \gamma\left(\partial_z\left(\alpha\sigma\Gamma^2\bar{p}\bar{u}p_{zx}^{(1)} + \alpha\sigma\Gamma^2\bar{p}v^{(1)}\bar{p}_{zy}\right)\right) + \gamma^2\left(\partial_z\left(\alpha\sigma\Gamma^2 p^{(1)}\bar{u}p_{zx}^{(1)}\right.\right.$$
$$\left.\left. + \alpha\sigma\Gamma^2\bar{p}\vec{\mathbf{u}}^{(1)}\cdot\nabla p_z^{(1)} + \alpha\sigma\Gamma^2 v^{(1)}\bar{p}_{zy} + \alpha\sigma\Gamma^2\bar{p}\bar{u}p_{zx}^{(2)} + \alpha\sigma\Gamma^2\bar{p}v^{(2)}\bar{p}_{zy}\right)\right)$$

$$-b = \gamma\left(\bar{p}_z w^{(1)}\right) + \gamma^2\left(p_z^{(1)}w^{(1)} + \bar{p}_z w^{(2)}\right)$$

$$\dot{A} = \Delta F_A + b \tag{A3}$$

$$\dot{A} = \gamma\left(\partial_t\left(\sigma\Gamma^2\bar{p}_z p_z^{(1)}\right)\right) + \gamma^2\left(\partial_t\left(\sigma\Gamma^2\frac{p^{(1)^2}}{2}\right) + \partial_t\left(\sigma\Gamma^2\bar{p}_z p_z^{(2)}\right)\right)$$

$$\Delta F_A = -\gamma\left(\alpha\Gamma^2\sigma\bar{u}\ \partial_x\left(\bar{p}_z p_z^{(1)}\right) + \alpha\Gamma^2\sigma\vec{\mathbf{u}}^{(1)}\cdot\nabla\frac{(\bar{p}_z)^2}{2}\right)$$

$$-\gamma^2\left(\alpha\Gamma^2\sigma\bar{u}\ \partial_x\left(\frac{p_z^{(1)^2}}{2}\right) + \alpha\Gamma^2\sigma\bar{u}\ \partial_x\left(\bar{p}_z p_z^{(2)}\right)\right.$$

$$\left. + \alpha\Gamma^2\sigma\vec{\mathbf{u}}^{(1)}\cdot\nabla\left(\sigma\bar{p}_z p_z^{(1)}\right) + \alpha\Gamma^2\sigma v^{(2)}\ \partial_y\frac{(\bar{p}_z)^2}{2}\right)$$

We now proceed to eliminate from eqs. A2 and A3 the contribution of the terms containing the $\phi^{(2)}$ fields. To do so, we note that the consistent $O(\gamma^2)$ contributions to the vertical velocity equation 12 and vorticity balance equation 13 are

$$w^{(2)} = -\Gamma^2\sigma p_{zt}^{(2)} - \alpha\Gamma^2\sigma\bar{u}p_{zx}^{(2)} - \alpha\Gamma^2\sigma\vec{\mathbf{u}}^{(1)}\cdot\nabla p_z^{(1)} - \alpha\Gamma^2 v^{(2)}\sigma\bar{p}_{zy} \tag{A4}$$

$$\frac{\partial\nabla^2 p^{(2)}}{\partial t} + \alpha\bar{u}\ \partial_x\nabla^2 p^{(2)} - \alpha v^{(2)}\bar{u}_{yy} + \alpha\vec{\mathbf{u}}^{(1)}\cdot\nabla\nabla^2 p^{(1)} = w_z^{(2)} \tag{A5}$$

Multiplying (A5) by $-\bar{p}$ and (A4) by $\bar{p}_z$ we obtain

$$\bar{u}\frac{\partial}{\partial t}u^{(2)} = -\alpha\bar{u}\ \partial_x\left(u^{(2)}\bar{u}\right) - \alpha\bar{u}\vec{\mathbf{u}}^{(1)}\cdot\nabla u^{(1)} - \alpha\vec{\mathbf{u}}^{(2)}\cdot\nabla\left(\frac{\bar{u}^2}{2}\right)$$

$$+\nabla\cdot\left(\bar{p}\nabla p_t^{(2)}\right) + \nabla\cdot\left(\bar{p}\alpha\bar{u}\ \partial_x\nabla p^{(2)}\right) + \partial_y\left(\bar{p}\alpha v^{(2)}\bar{p}_{yy}\right)$$

$$+\nabla\cdot\left(\bar{p}\alpha\vec{\mathbf{u}}^{(1)}\cdot\nabla\nabla p^{(1)}\right) + \partial_z\left(\bar{p}\Gamma^2\sigma p_{zt}^{(2)}\right)$$

$$+\partial_z\left(\bar{p}\alpha\bar{u}\Gamma^2\sigma p_{zx}^{(2)} + \bar{p}\alpha\Gamma^2\sigma\vec{\mathbf{u}}^{(1)}\cdot\nabla p_z^{(1)} + \bar{p}v^{(2)}\alpha\Gamma^2\sigma\bar{p}_{zy}\right) + \bar{p}_z w^{(2)} \tag{A6}$$

$$\sigma\Gamma^2\bar{p}_z\frac{\partial}{\partial t}p_z^{(2)} = -\alpha\Gamma^2\sigma\bar{u}\ \partial_x\left(\bar{p}_z p_z^{(2)}\right) - \alpha\Gamma^2\sigma\bar{p}_z\vec{\mathbf{u}}^{(1)}\cdot\nabla p_z^{(1)}$$

$$-\alpha\Gamma^2\sigma v^{(2)}\ \partial_y\frac{(\bar{p}_z)^2}{2} - \bar{p}_z w^{(2)} \tag{A7}$$

We next subtract the lfs (rhs) of A6 from the lfs (rhs) of A2 and similarly for

A7 and A3. All $\phi^{(2)}$ terms cancel and there results:
to $O(\gamma)$

$$\dot{K}^{(1)} = -\bar{u}\,\partial_x(u^{(1)}\bar{u}) - \vec{\mathbf{u}}^{(1)}\cdot\nabla\frac{\bar{u}^2}{2} + \nabla\cdot\left(\bar{p}\,\nabla p_t^{(1)}\right) + \nabla\cdot\left(\bar{p}\bar{u}\,\partial_x\nabla p^{(1)}\right)$$
$$+\nabla\cdot\left(\bar{p}\vec{\mathbf{u}}^{(1)}\cdot\nabla\nabla\bar{p}\right) + \partial_z\left(\bar{p}\Gamma^2\sigma p_{zt}^{(1)}\right)$$
$$+\partial_z\left(\bar{p}\alpha\Gamma^2\sigma\bar{u}p_{zx}^{(1)} + \bar{p}\alpha\Gamma^2\sigma v^{(1)}\bar{p}_{zy}\right) + \bar{p}_z w^{(1)} \qquad \text{(A8)}$$

$$\dot{A}^{(1)} = -\alpha\sigma\Gamma^2\bar{u}\,\partial_x\left(\bar{p}_z p_z^{(1)}\right) - \alpha\Gamma^2\sigma\vec{\mathbf{u}}^{(1)}\cdot\nabla\left(\frac{\bar{p}^2}{2}\right) - \bar{p}_z w^{(1)} \qquad \text{(A9)}$$

to $O(\gamma^2)$

$$\dot{K}^{(2)} = -\alpha\bar{u}\,\partial_x K^{(2)} - u^{(1)}v^{(1)}\bar{u}_y + \nabla\cdot\left(p^{(1)}\,\nabla p_t^{(1)}\right)$$
$$+\nabla\cdot\left(p^{(1)}\alpha\bar{u}\,\partial_x\nabla p^{(1)} + \alpha p^{(1)}v^{(1)}\bar{p}_{yy}\hat{j}\right) + \partial_z\left(\sigma\Gamma^2 p^{(1)}p_{zt}^{(1)}\right)$$
$$+\partial_z\left(\alpha\Gamma^2\sigma p^{(1)}\bar{u}p_{zx}^{(1)} + \alpha\Gamma^2\sigma p^{(1)}v^{(1)}\bar{p}_{zy}\right) + p_z^{(1)}w^{(1)} \qquad \text{(A10)}$$

$$\dot{A}^{(2)} = -\alpha\bar{u}\,\partial_x A^{(2)} - \alpha\Gamma^2\sigma p_z^{(1)}v^{(1)}\bar{p}_{zy} - p_z^{(1)}w^{(1)} \qquad \text{(A11)}$$

where $K^{(1)} = \bar{u}u^{(1)}$, $A^{(1)} = \sigma\Gamma^2\bar{p}_z p_z^{(1)}$ and $K^{(2)} = 1/2(u^{(1)2} + v^{(1)2})$, $A^{(2)} = 1/2\sigma\Gamma^2(p_z^{(1)})^2$. The elimination of the $\phi^{(2)}$ fields has produced 'Reynolds' stress and heat flux like terms, the well known source of barotropic-baroclinic instabilities, in ΔF_κ, ΔF_A and they appear in the $O(\gamma^2)$ equations. The δf_π^a, ΔF_π^a terms in the $O(\gamma^2)$ equations are left with a pressure energy flux due to correlation between $p^{(1)}v^{(1)}$ fields weighted by horizontal and vertical shear of the mean flow. We will see that the $O(\gamma)$ equations only represent redistribution of energy in the field which essentially averages to zero in time everywhere.

REFERENCES

Bray, N.A. and Fofonoff, N.P., 1981. Available potential energy for mode eddies. J. Phys. Oceanogr., 11: 30–47.

Bryden, H.L., 1982. Sources of eddy energy in the Gulf Stream recirculation region. J. Mar. Res., 40: 1047–1068.

Eady, E.T., 1949. Long waves and cyclone waves. Tellus, 1: 258–277.

Gill, A.E., 1982. Atmosphere-Ocean Dynamics. Academic Press, Vol. 30, p. 565.

Haidvogel, D.B. and Holland, W.R., 1978. The stability of ocean currents in eddy-resolving general circulation models. J. Phys. Oceanogr., 8: 393–413.

Harrison, D.E., 1979. Eddies and the general circulation of numerical model gyres: an energetic perspective. Rev. of Geophys. Space Phys., 17: 969–979.

Harrison, D.E. and Robinson, A.R., 1978. Energy analysis of open regions of turbulent flows-mean eddy energetics of a numerical ocean circulation experiment. Dyn. Atmos. Oceans, 2: 185–211.

Holliday, D. and McIntyre, M.E., 1981. On potential energy density in an incompressible, stratified fluid. J. Fluid Mech., 107: 221–225.
Longuet-Higgins, M.S., 1964. On group velocity and energy flux in planetary wave motion. Deep-Sea Res., 11: 35–42.
Lorenz, E.N., 1955. Available potential energy and the maintenance of the general circulation. Tellus, 7: 157–167.
Lorenz, E.N., 1967. The nature and theory of the general circulation on the atmosphere. World Meterological Organization, 161 pp.
McWilliams, J.C. et al., 1983. The local dynamics of eddies in the western North Atlantic. In: A.R. Robinson (Editor), Eddies In Marine Sciences. Springer-Verlag, Chapter 5.
Miller, R.N., Robinson, A.R. and Haidvogel, D.B., 1983. A baroclinic quasigeostrophic open ocean model. J. Comp. Phys., 50: 38–70.
Pedlosky, J., 1979. Geophysical Fluid Dynamics. Springer-Verlag, pp. 346.
Plumb, R.A., 1983. A new look at the energy cycle. J. Atmos. Sci., 40: 1669–1688.
Plumb, R.A., 1985. An alternative form of Andrew's conservation law for quasigeostrophic waves on a steady, nonuniform flow. J. Atmos. Sci., 42: 298–300.
Robinson, A.R. and Leslie, W.G., 1985. Estimation and prediction of oceanic eddy fields. Prog. Oceanog., 14: 485–510.
Robinson, A.R., Carton, J.A., Mooers, C.N.K., Walstad,, L.J., Carter, E.F., Rienecker, M.M., Smith, J.A. and Leslie, W.G., 1985a. A real time dynamical forecast of ocean synoptic/mesoscale eddies. Nature, 309: 781–783.
Robinson, A.R., Carton, J.A., Pinardi, N. and Mooers, C.N.K., 1986. Dynamical forecasting and dynamical interpolation: an experiment in the California current. Submitted to J. Phys. Oceanogr.
Van Mieghem, J., 1973. Atmospheric Energetics. Clarendon Press, Oxford, 306 pp.